Constraining Tropospheric Stability using Surface Temperature Patterns: A Machine Learning Approach

Li-Wei Chao, Mark Zelinka, Stephen Po-Chedley

Lawrence Livermore National Laboratory

Confronting Earth System Model Trends with Observations: The Good, the Bad, and the Ugly

March 15, 2024

This work was supported by the U.S. Department of Energy (DOE) Regional and Global Model Analysis program area. This work was performed under the auspices of the DOE by Lawrence Livermore National Laboratory under Contract DE-AC52-07NA27344. LLNL-PRES-861529

We gratefully acknowledge support from DOE's Regional and Global Model Analysis Program Area

PCMDI

Earth System Model Evaluation Project

Motivations

- Cloud feedback depends not just on global mean surface temperature, but also on tropospheric stability (estimated inversion strength, EIS), which itself governed by the evolving spatial patterns of surface warming.

  → Pattern Effect

Motivations

- Cloud feedback depends not just on global mean surface temperature, but also on tropospheric stability (estimated inversion strength, EIS), which itself governed by the evolving spatial patterns of surface warming.

  → Pattern Effect

- Quantifying the strength of pattern effect is a crucial step to constrain the cloud feedback (and climate sensitivity) using historical record

Motivations

- Cloud feedback depends not just on global mean surface temperature, but also on tropospheric stability (estimated inversion strength, EIS), which itself governed by the evolving spatial patterns of surface warming.

  → Pattern Effect

- Quantifying the strength of pattern effect is a crucial step to constrain the cloud feedback (and climate sensitivity) using historical record
- Understanding how EIS responds to warming is thus critical

Motivations
Pattern Effect & EIS

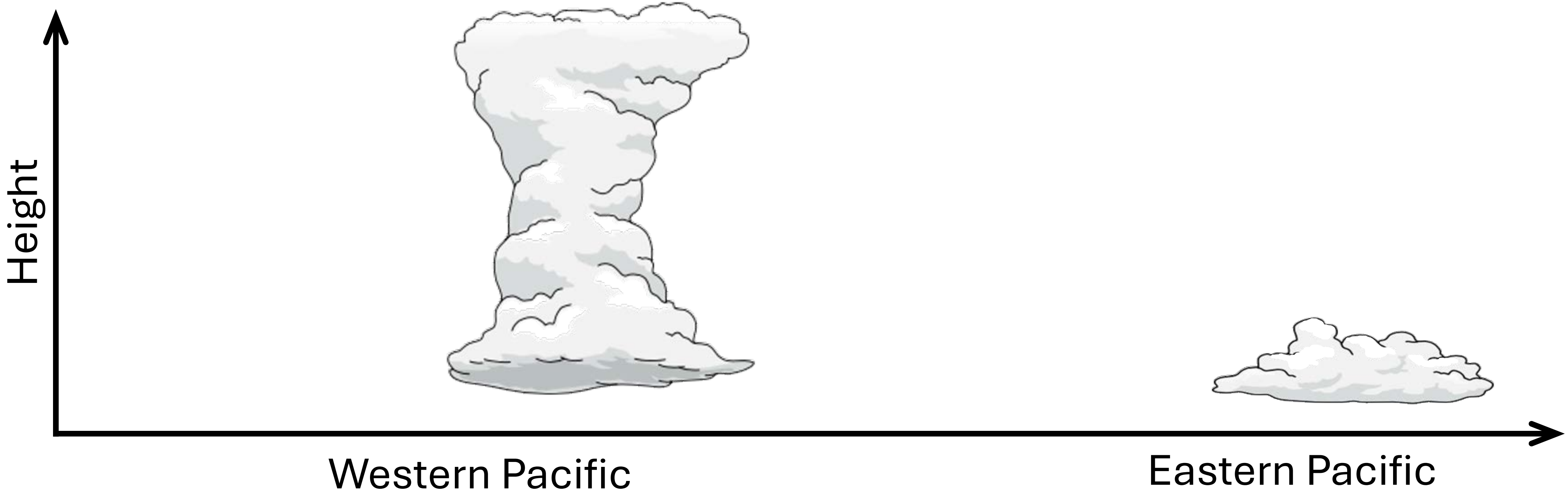

(Zhou et al., 2016, 2017, Mauritsen, 2016,
Andrews and Webb, 2018, Dong et al., 2019, etc)

Motivations Pattern Effect & EIS

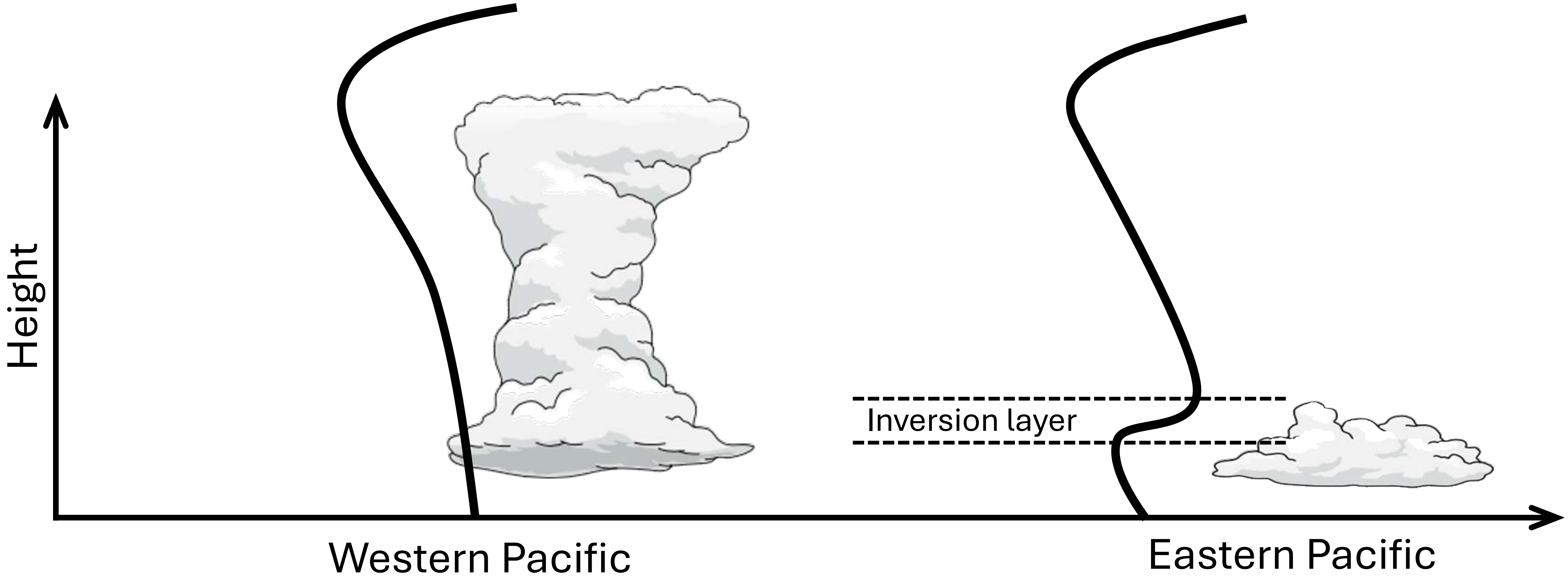

(Zhou et al., 2016, 2017, Mauritsen, 2016,
Andrews and Webb, 2018, Dong et al., 2019, etc)

Motivations Pattern Effect & EIS

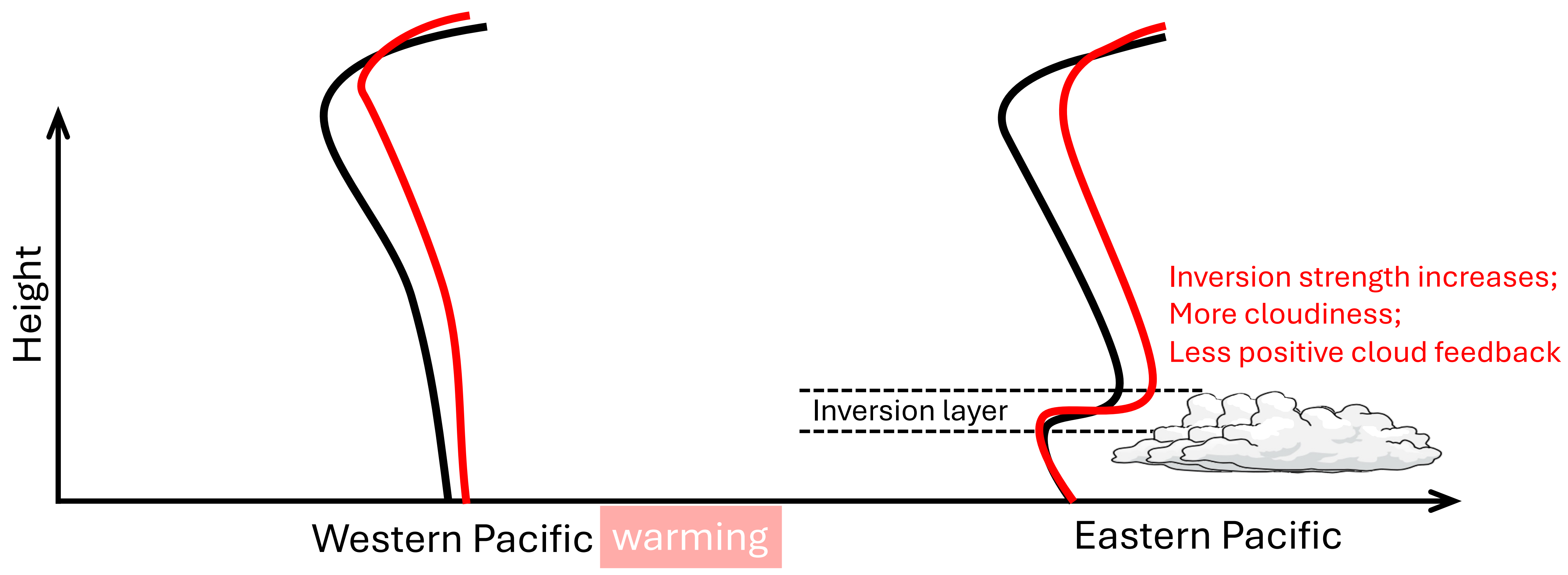

(Zhou et al., 2016, 2017, Mauritsen, 2016,
Andrews and Webb, 2018, Dong et al., 2019, etc)

Motivations Pattern Effect & EIS

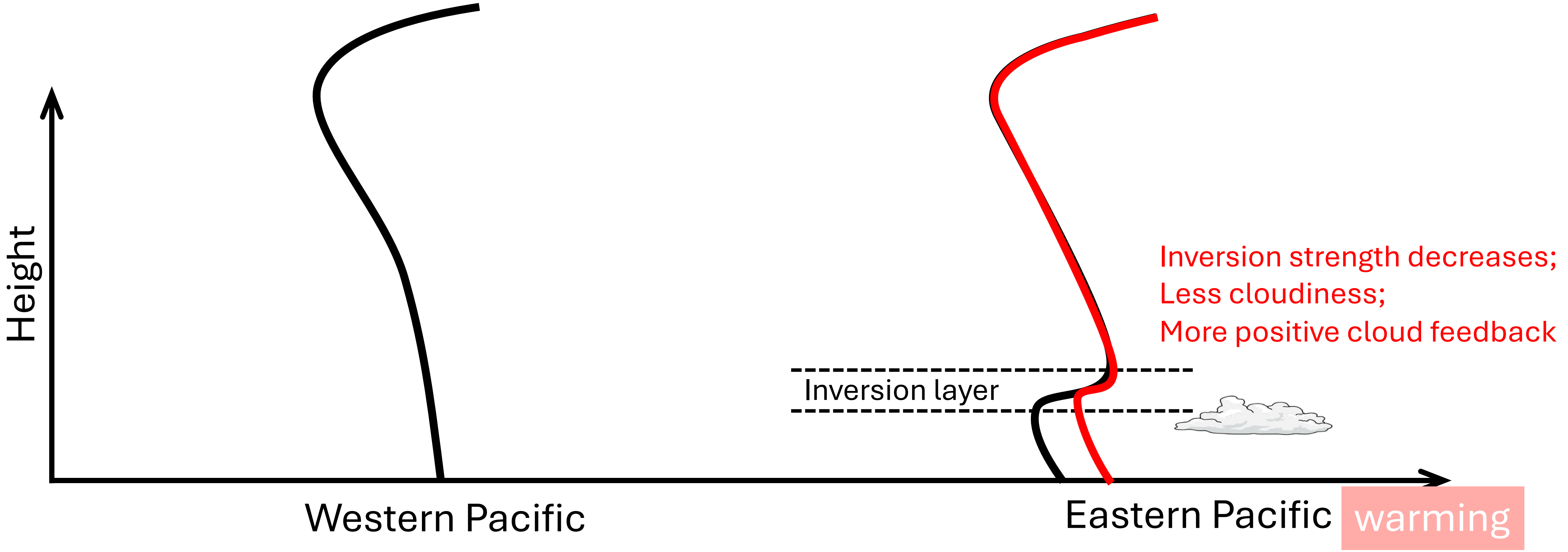

(Zhou et al., 2016, 2017, Mauritsen, 2016,
Andrews and Webb, 2018, Dong et al., 2019, etc)

Motivations Low Cloud Feedback Pattern Effect vs. dEIS/dT

*dT = global average near-surface air temperature

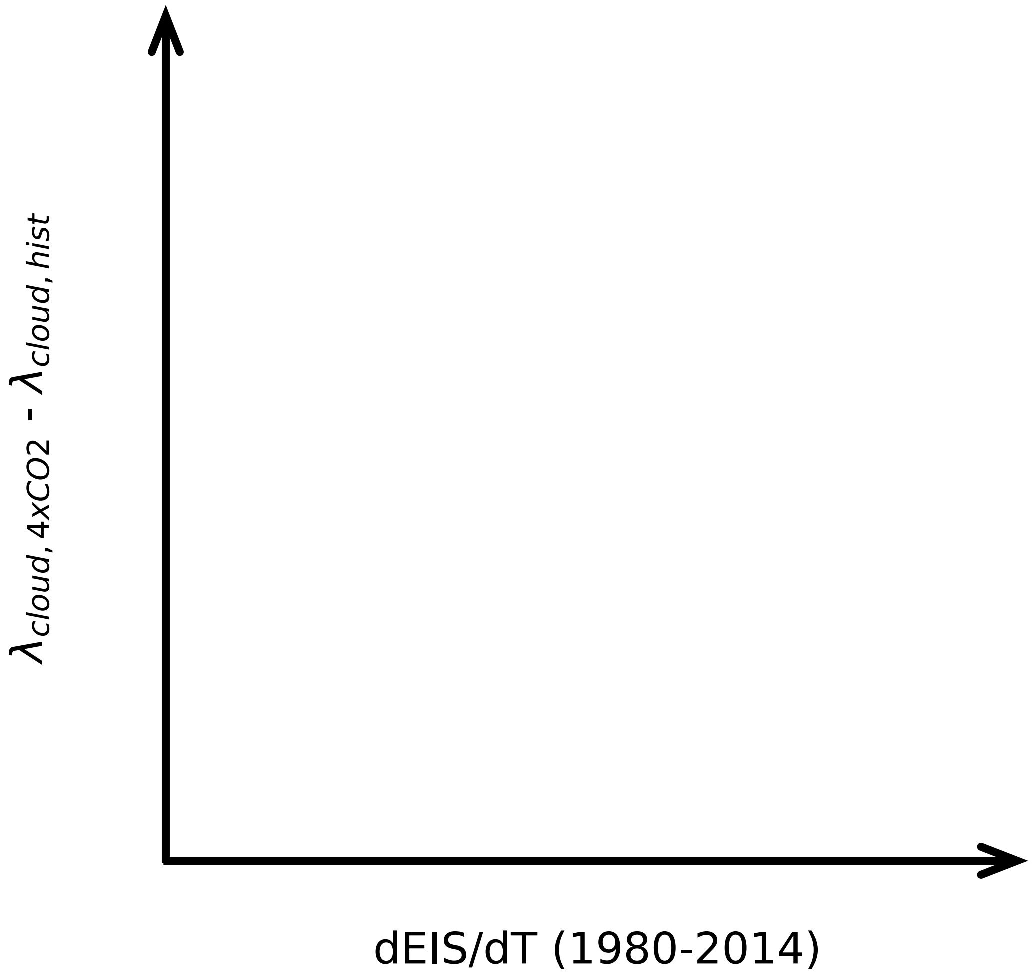

Motivations Low Cloud Feedback Pattern Effect vs. dEIS/dT

*dT = global average near-surface air temperature

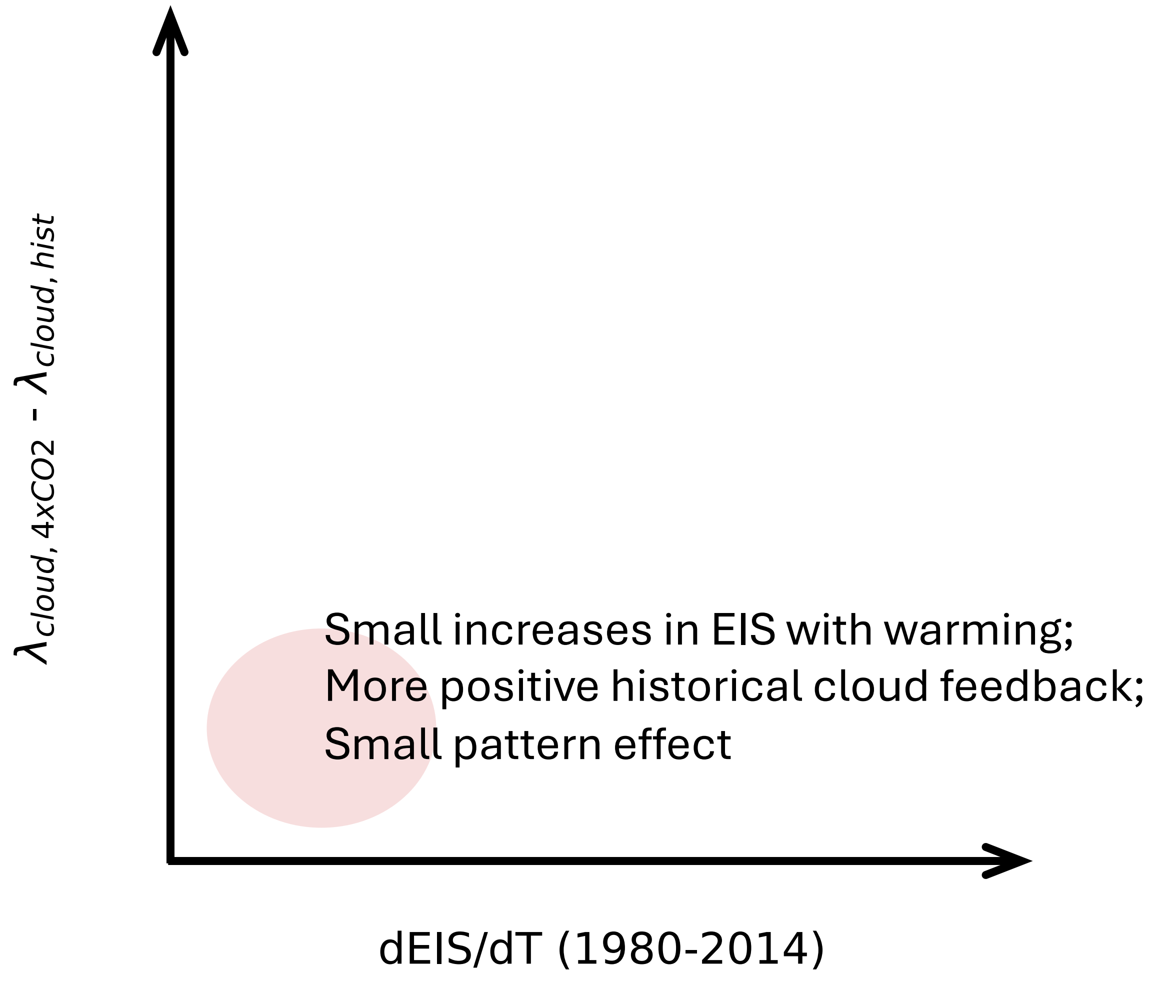

Motivations Low Cloud Feedback Pattern Effect vs. dEIS/dT

*dT = global average near-surface air temperature

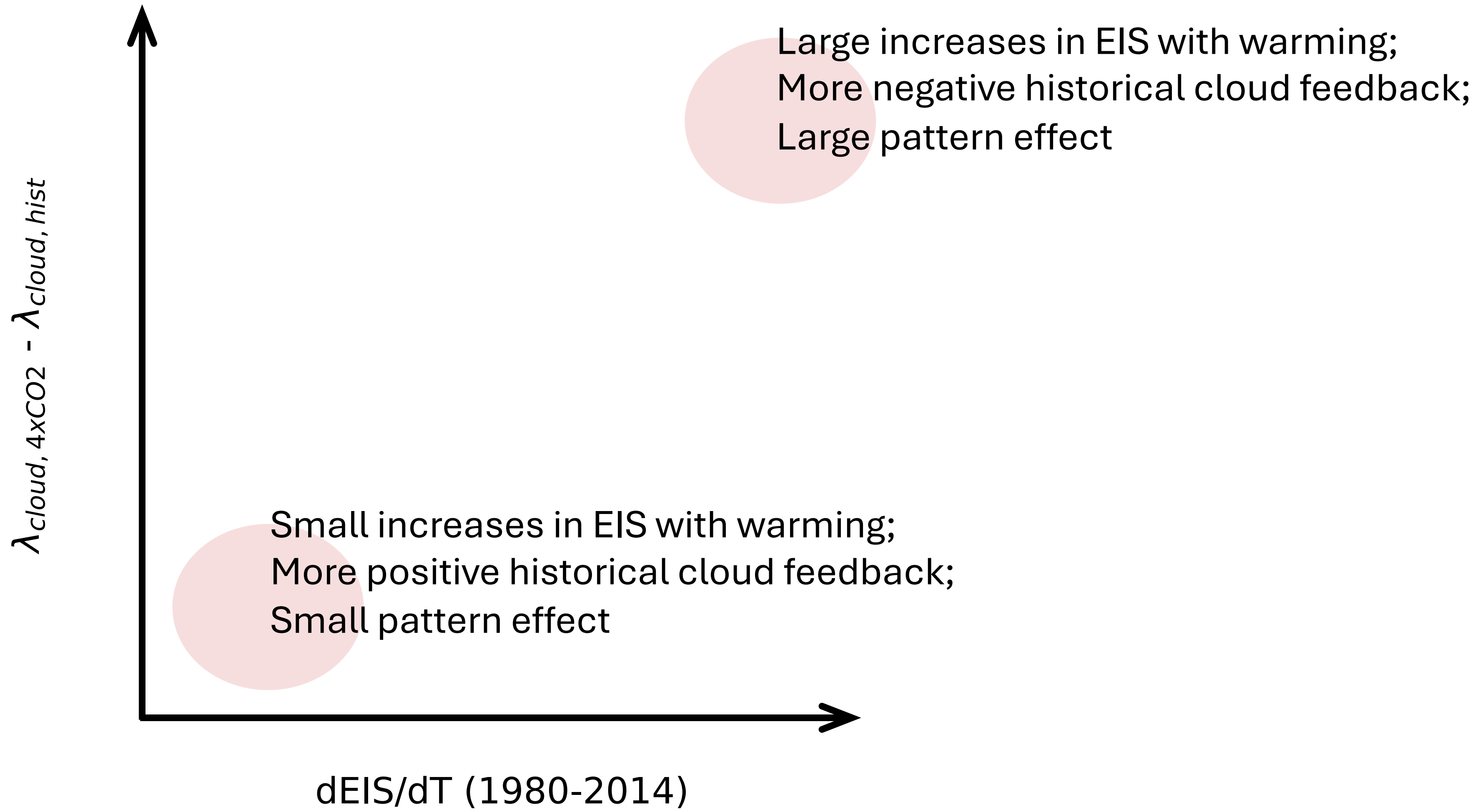

Motivations Low Cloud Feedback Pattern Effect vs. dEIS/dT

*dT = global average near-surface air temperature

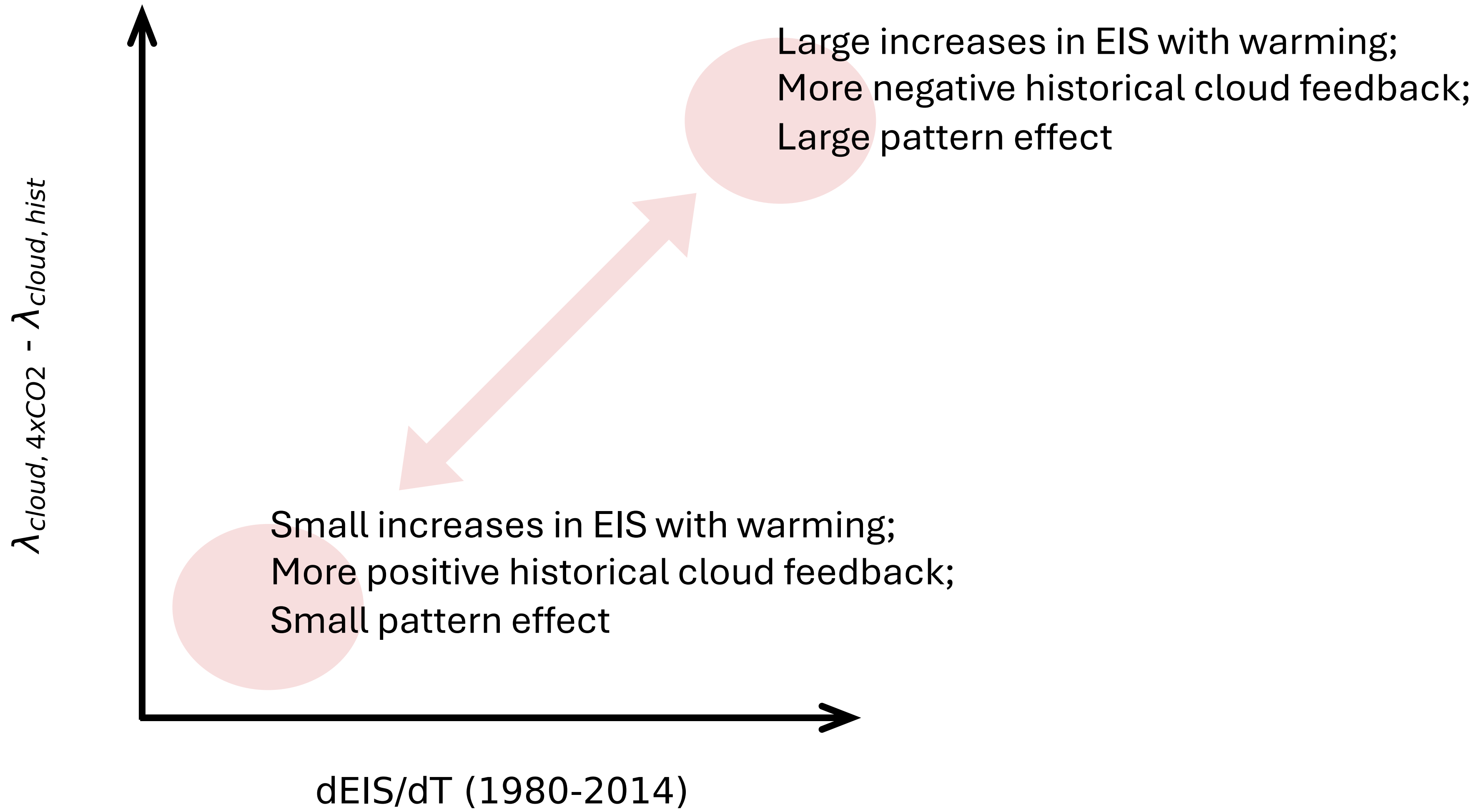

Motivations Low Cloud Feedback Pattern Effect vs. dEIS/dT

*dT = global average near-surface air temperature

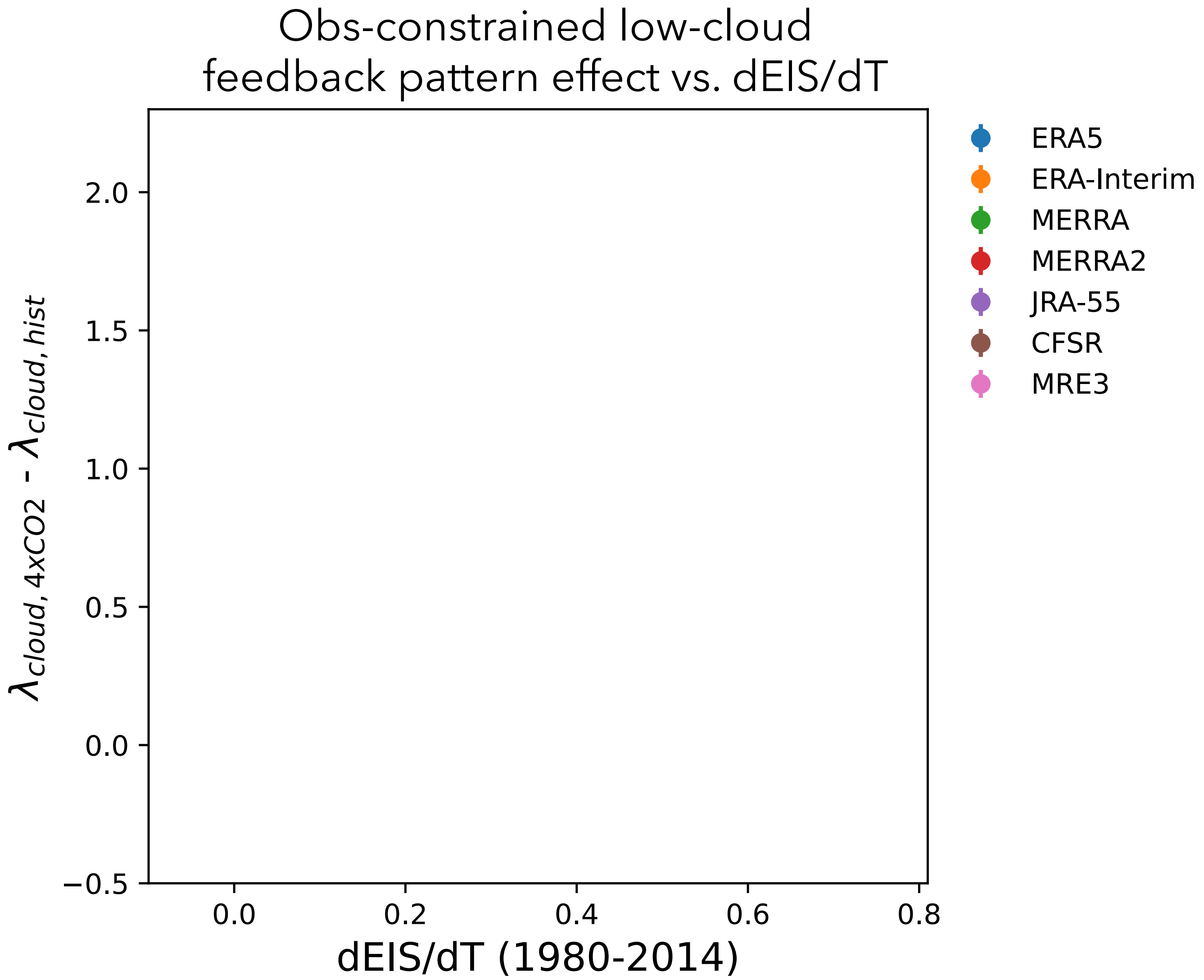

Modified from Myers et al. (2023)

Motivations Low Cloud Feedback Pattern Effect vs. dEIS/dT

*dT = global average near-surface air temperature

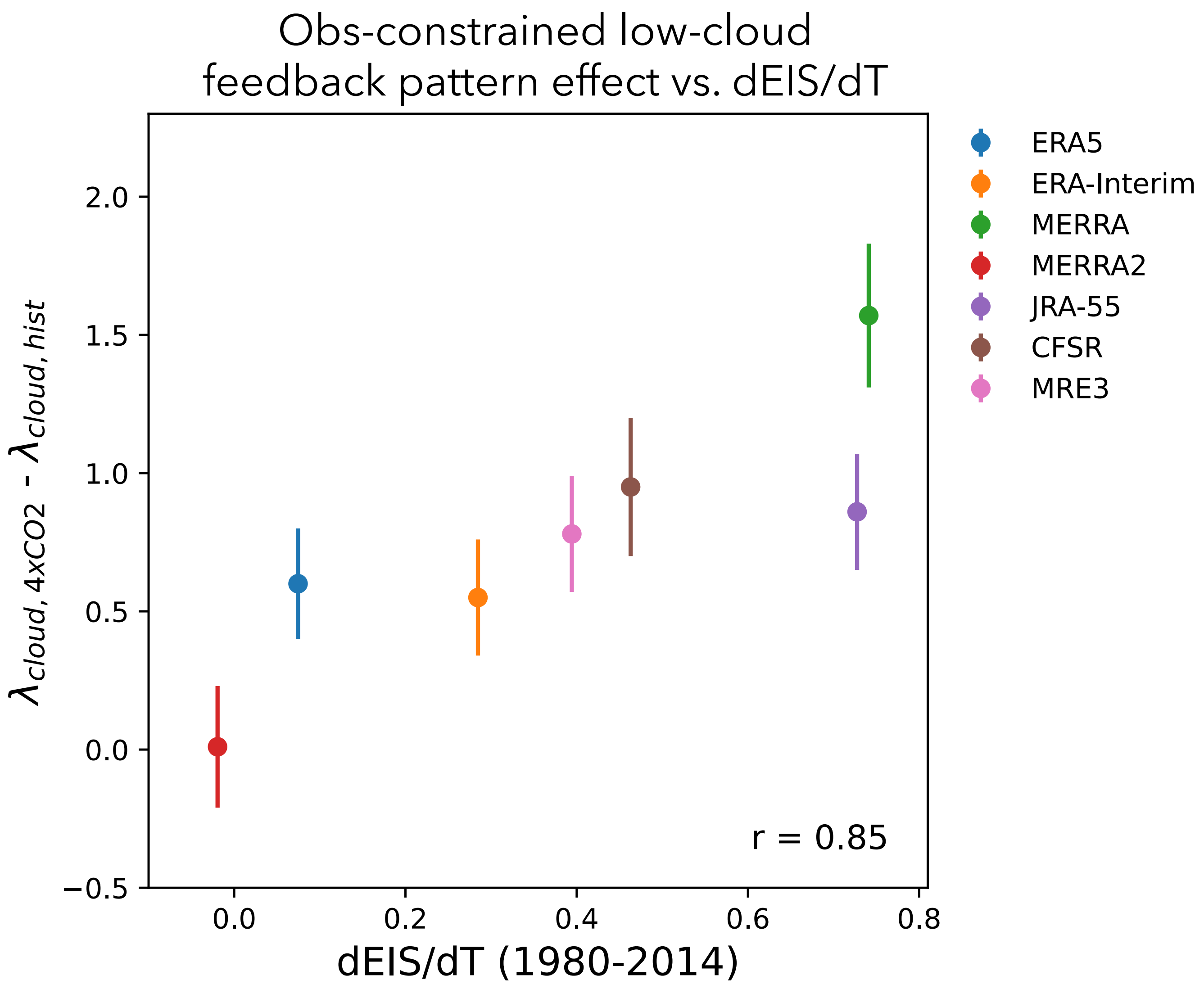

- The strength of pattern effect is correlated with the changes of EIS with warming
- The estimations of dEIS/dT vary widely among different reanalysis datasets (-0.02 to 0.74 K/K), limiting the ability to constrain the pattern effect

Considerations:

- Po-Chedley et al. (2022) found that machine learning could accurately predict mid-troposphere temperature given the surface temperature pattern

Modified from Myers et al. (2023)

Motivations
Low Cloud Feedback Pattern Effect vs. dEIS/dT

*dT = global average near-surface air temperature

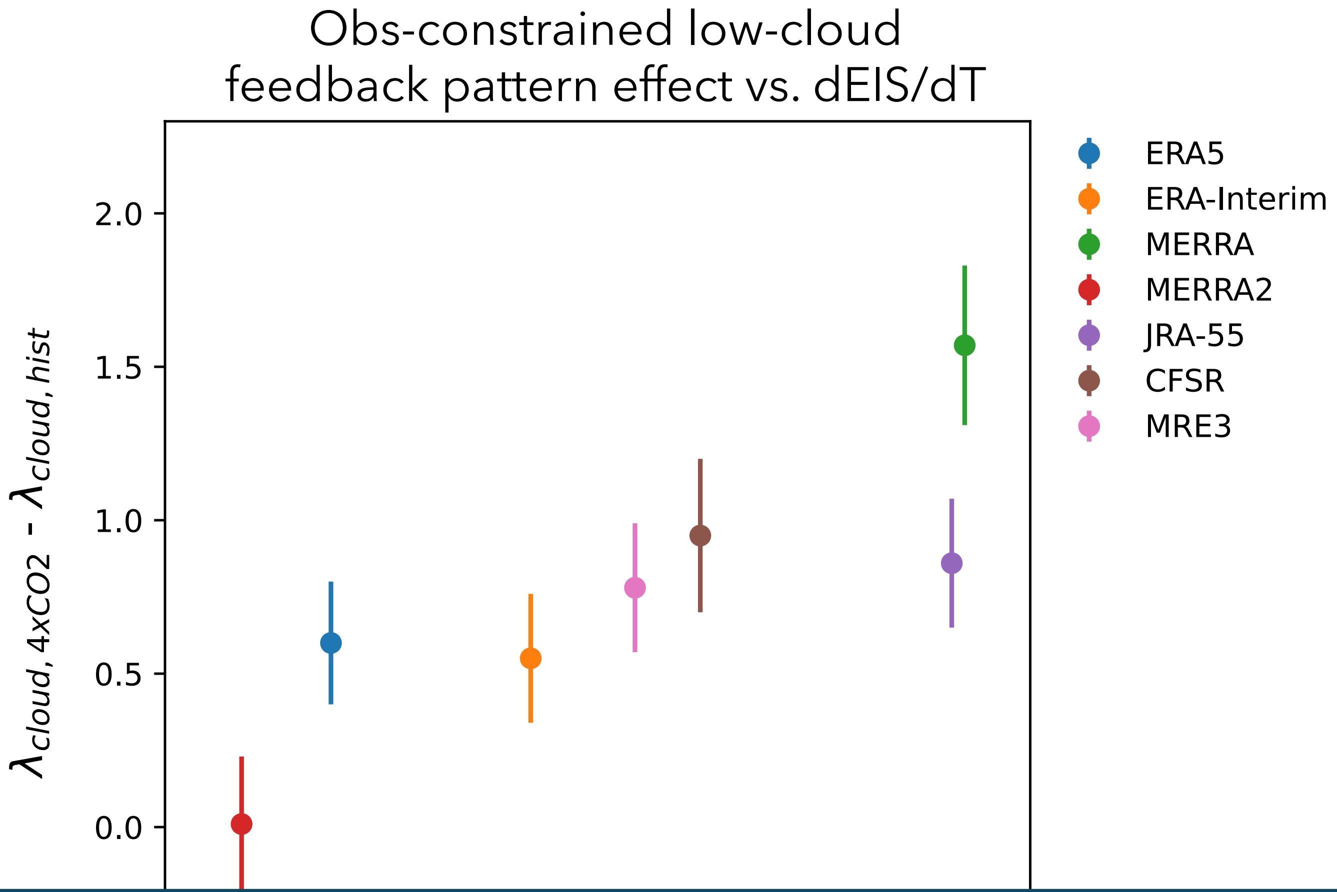

- The strength of pattern effect is correlated with the changes of EIS with warming
- The estimations of dEIS/dT vary widely among different reanalysis datasets (-0.02 to 0.74 K/K), limiting the ability to constrain the pattern effect

Considerations:

- Po-Chedley et al. (2022) found that machine learning could ccurately predict mid- osphere temperature given rface temperature pattern

Objectives:
Machine learning approach
(1) to relate surface warming pattern to EIS changes
(2) to gain insights into the reliability of reanalysis-derived EIS

Methods Machine learning (ML) with leave-one-out approach

Methods Machine learning (ML) with leave-one-out approach

Global Climate Models (GCMs) (9 models)

- 9 CMIP6 models that have at least 10 ensemble members
- Training period: 1979 – 2022 (historical + SSP3-7.0 simulations)
- Predictor: annual anomaly of global surface temperature pattern
- Predictand: annual anomaly of tropical-averaged EIS values

Methods Machine learning (ML) with leave-one-out approach

Global Climate Models (GCMs) (9 models)

Training dataset
(8 models)

Testing dataset
(1 model)

Methods Machine learning (ML) with leave-one-out approach

Global Climate Models (GCMs) (9 models)

Training dataset (8 models)

Predictor (input):
Annual anomaly of global surface temperature pattern

Predictand (output):
Annual anomaly of tropical EIS value

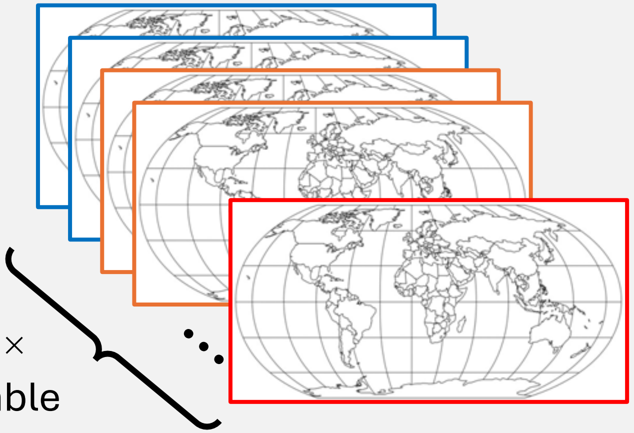

8 models ×
10 ensemble
members ×
N years

ML

Partial least squares (PLS)

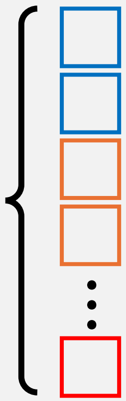

Testing dataset (1 model)

Methods Machine learning (ML) with leave-one-out approach

Predictor (input):
Annual anomaly of global
surface temperature pattern

Predictand (output):
Annual anomaly of
tropical EIS value

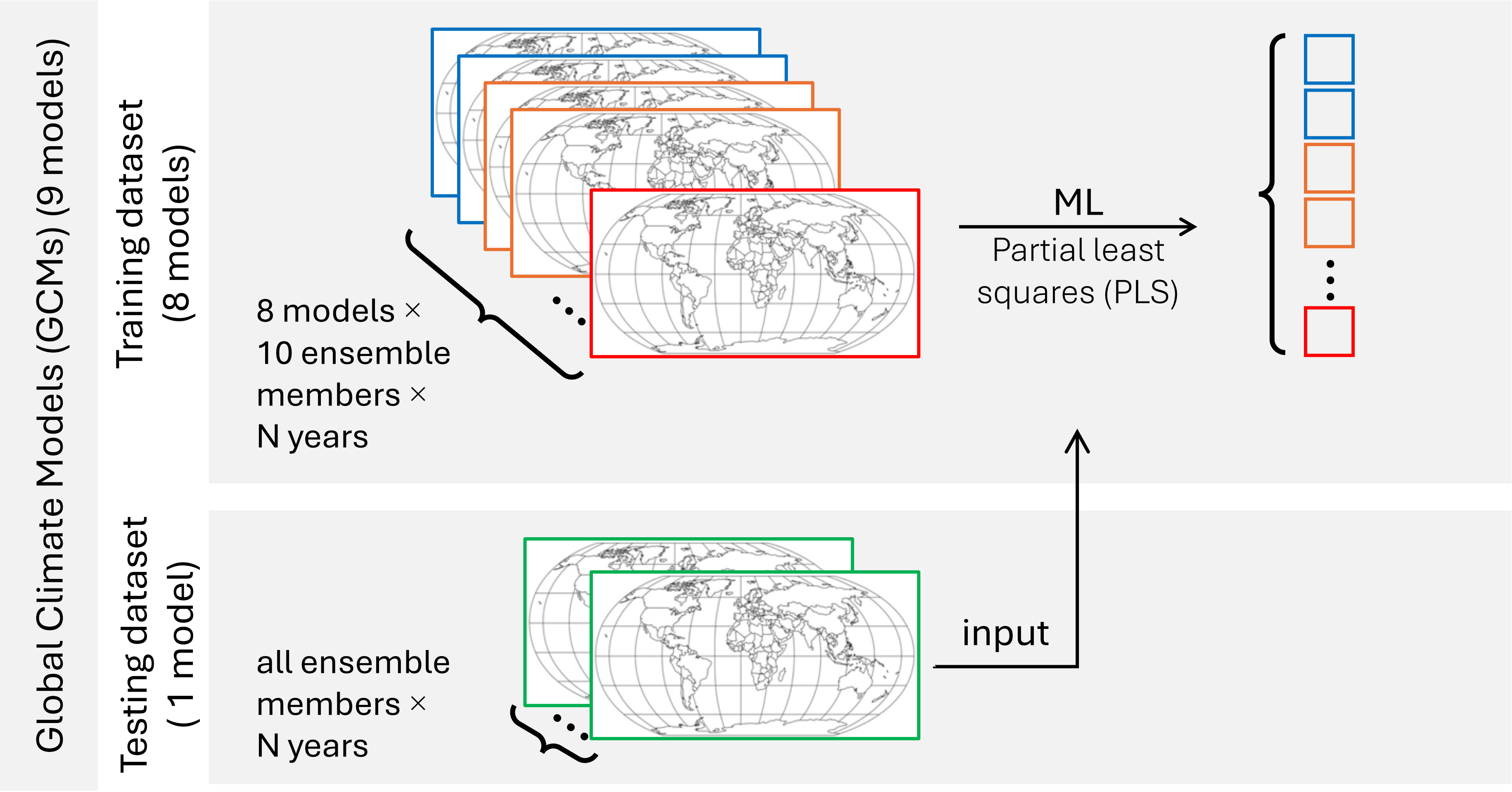

Methods Machine learning (ML) with leave-one-out approach

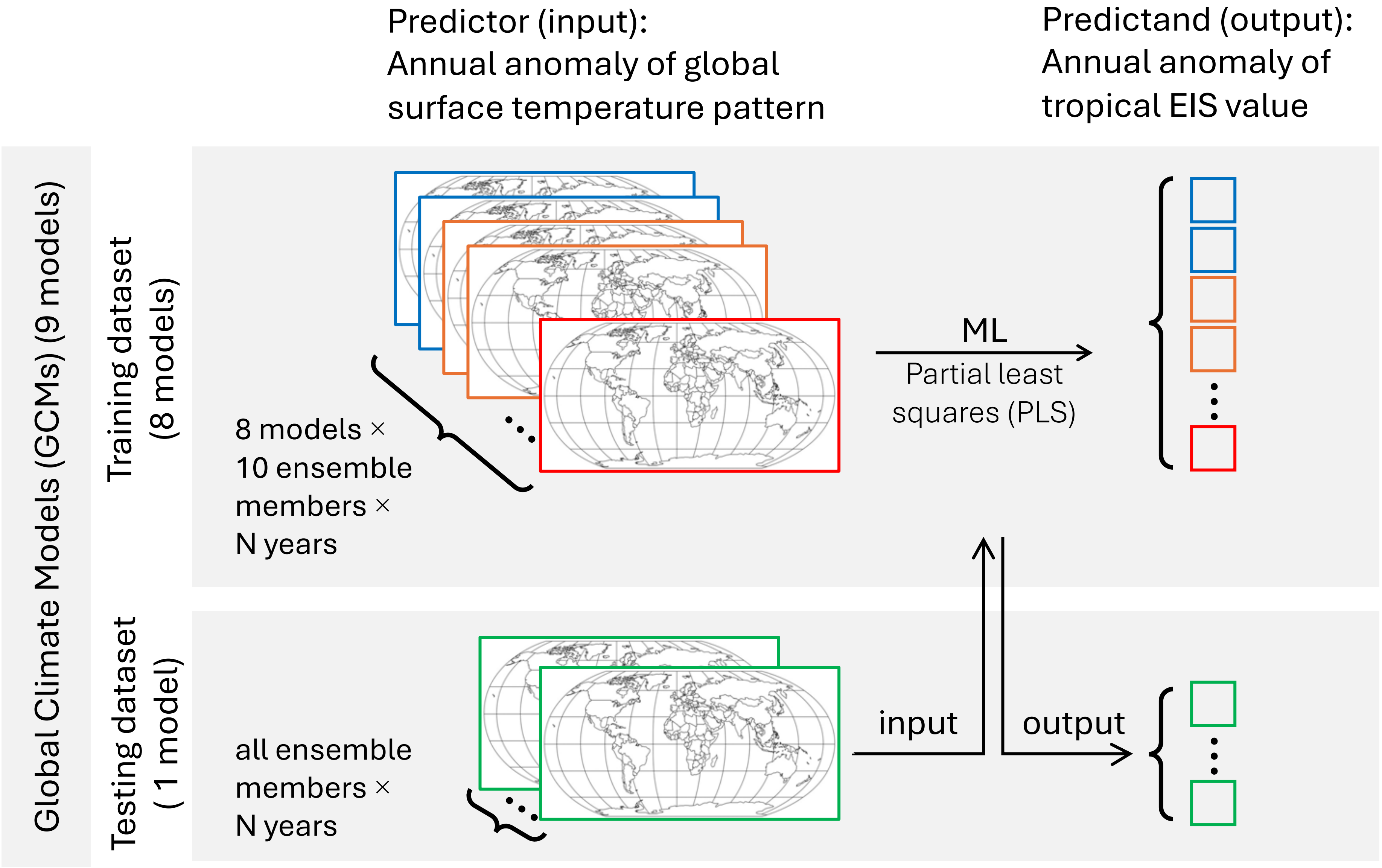

Methods Machine learning (ML) with leave-one-out approach

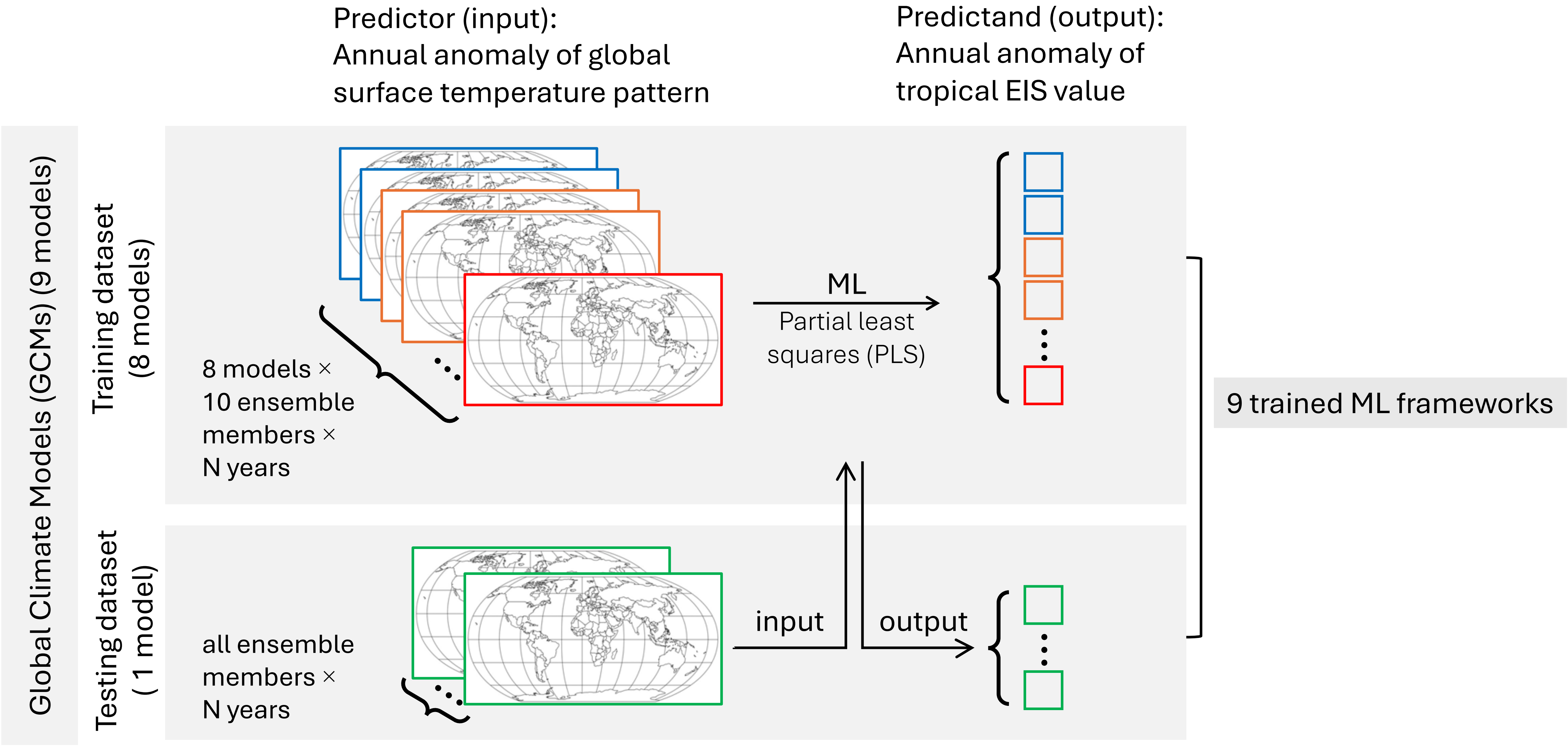

Methods Machine learning (ML) with leave-one-out approach

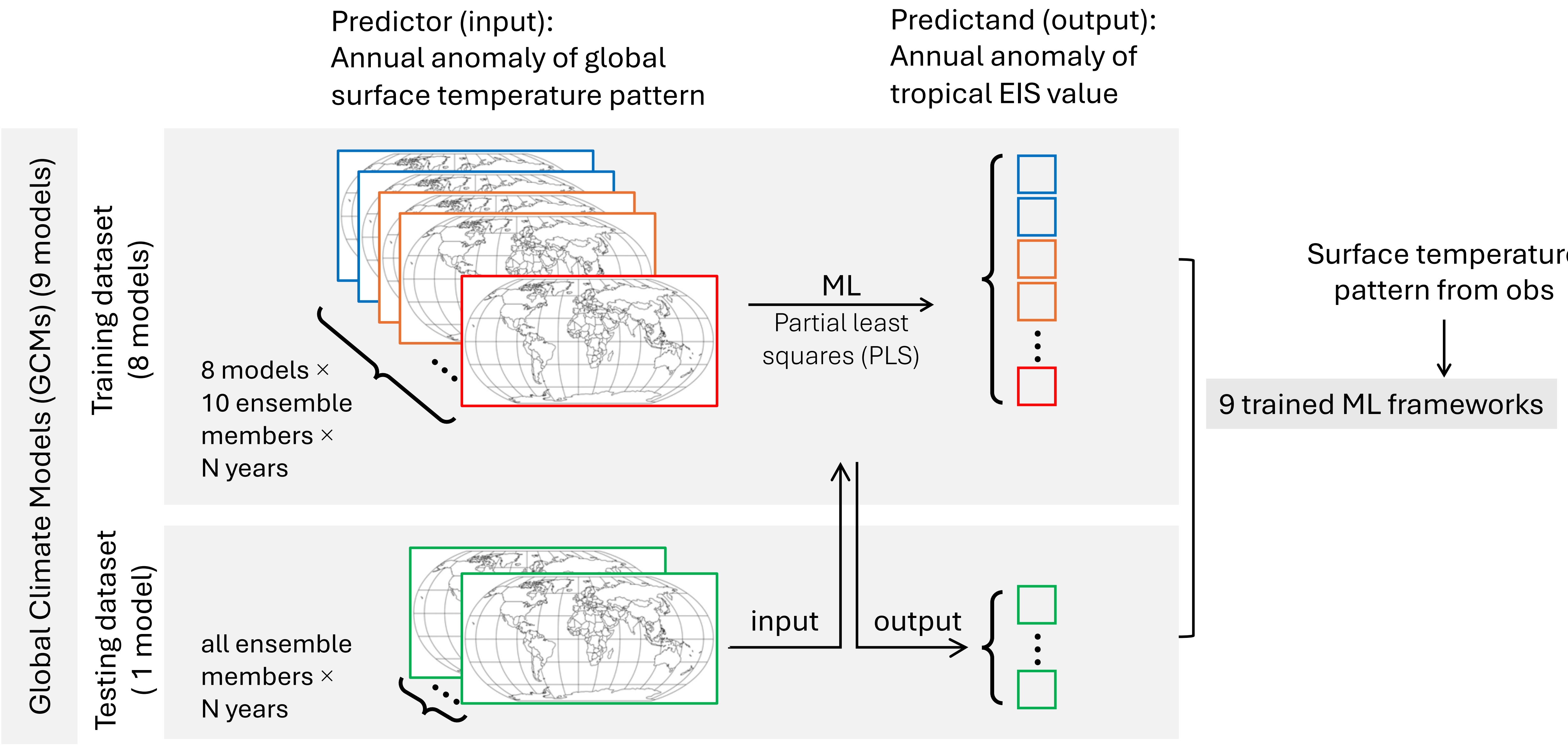

Methods Machine learning (ML) with leave-one-out approach

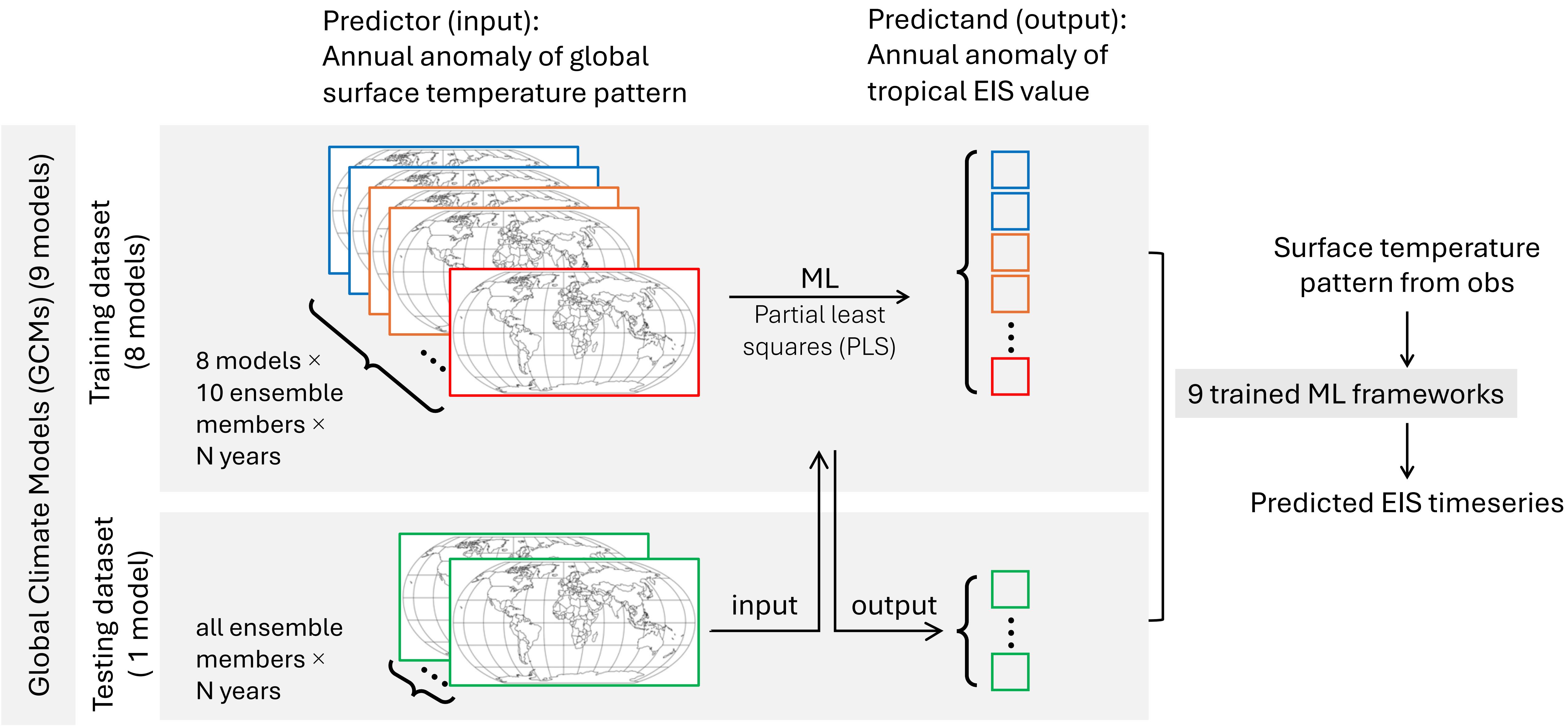

Methods Machine learning (ML) with leave-one-out approach

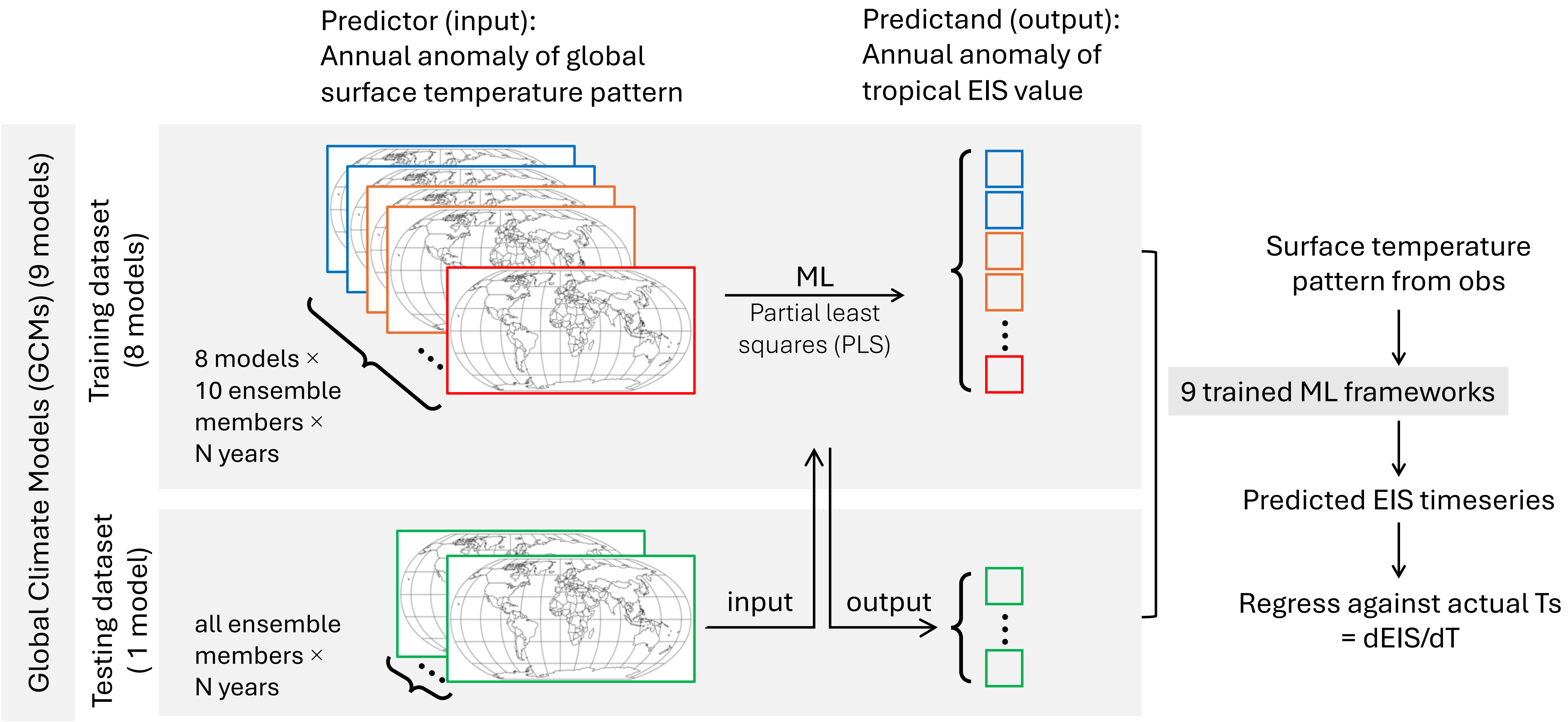

Results (1)

Predictor: Ts map

ML: PLS regression

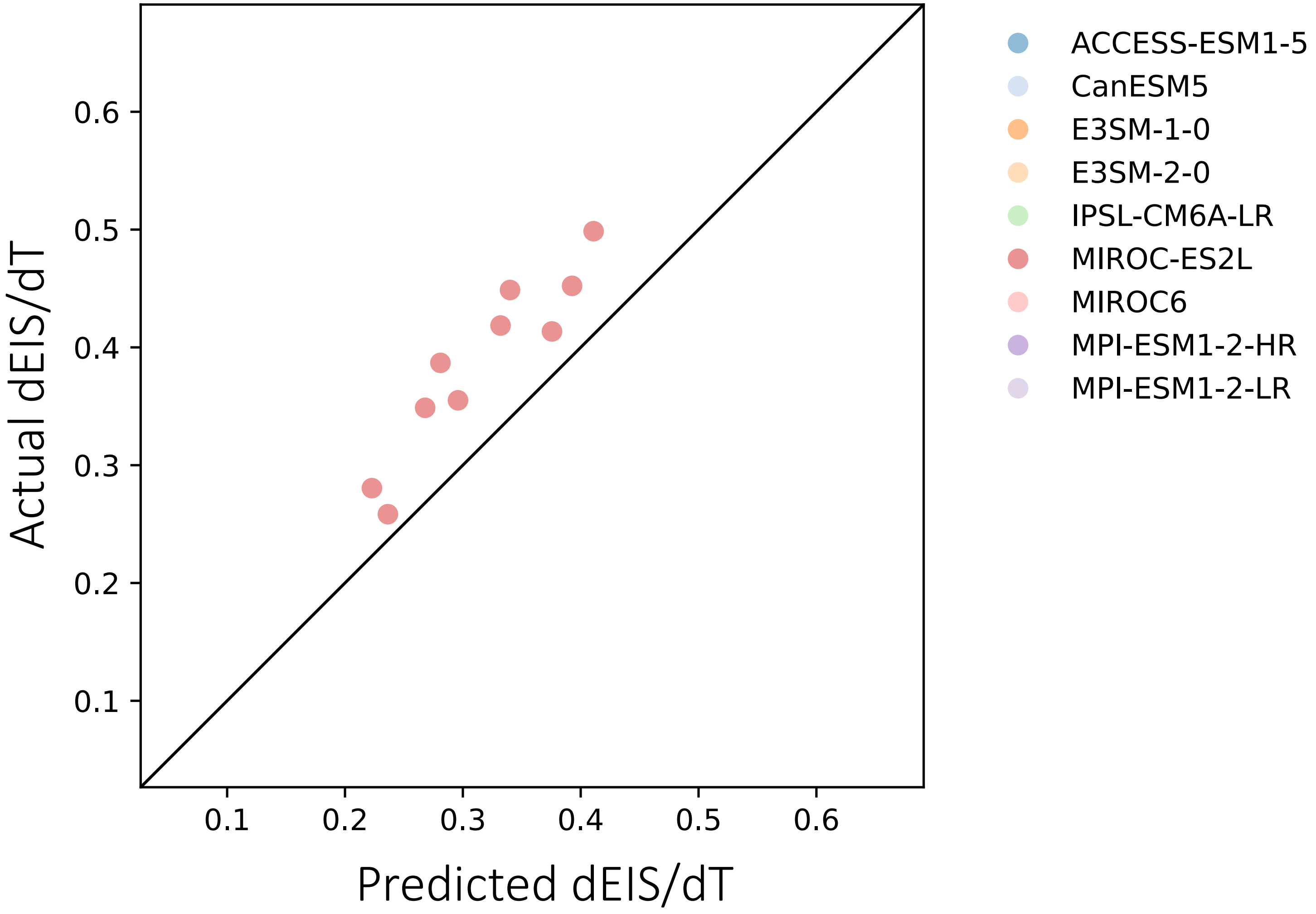

Results (1) dEIS/dT can be predicted by ML

Predictor: Ts map

ML: PLS regression

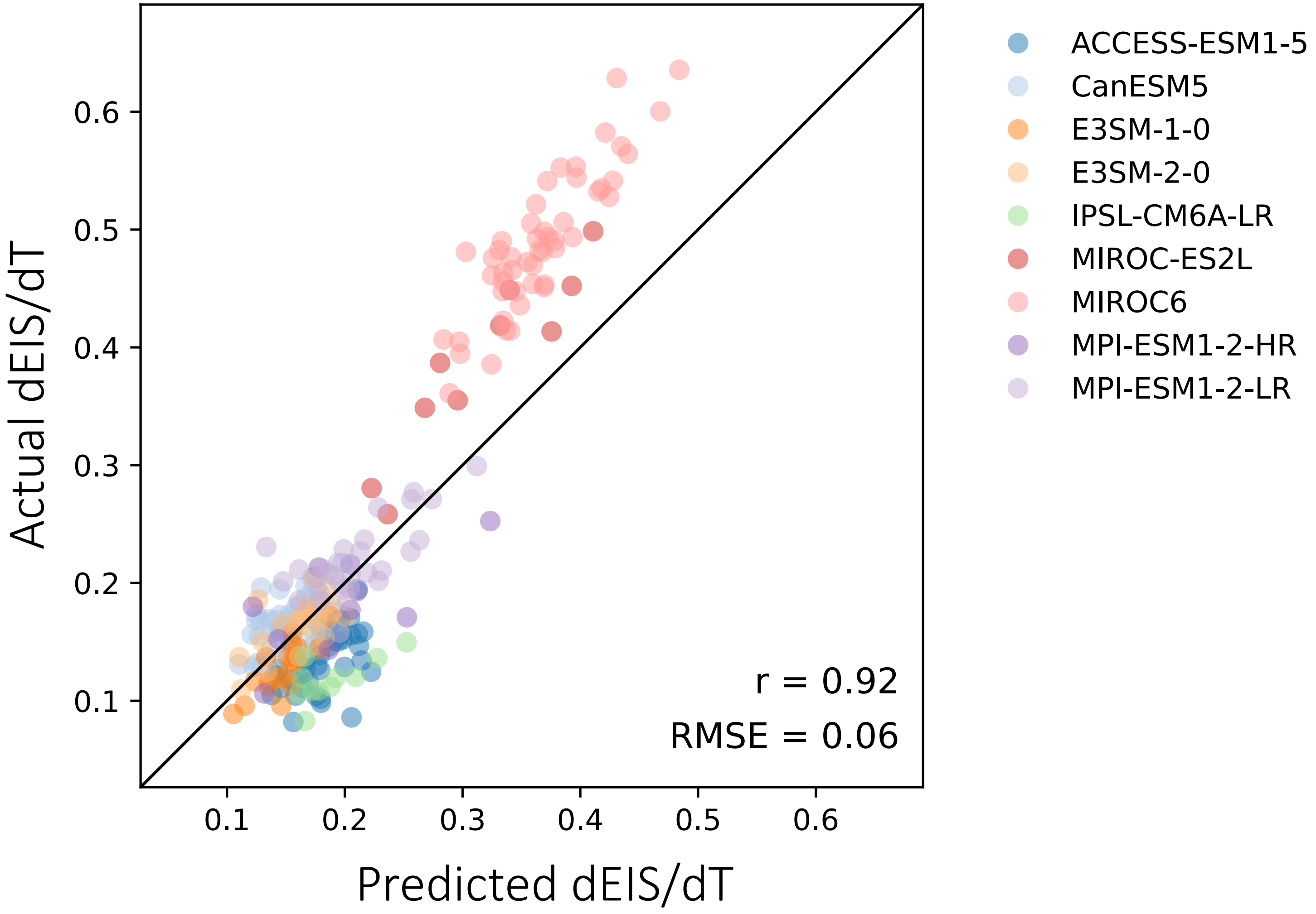

Results (2)

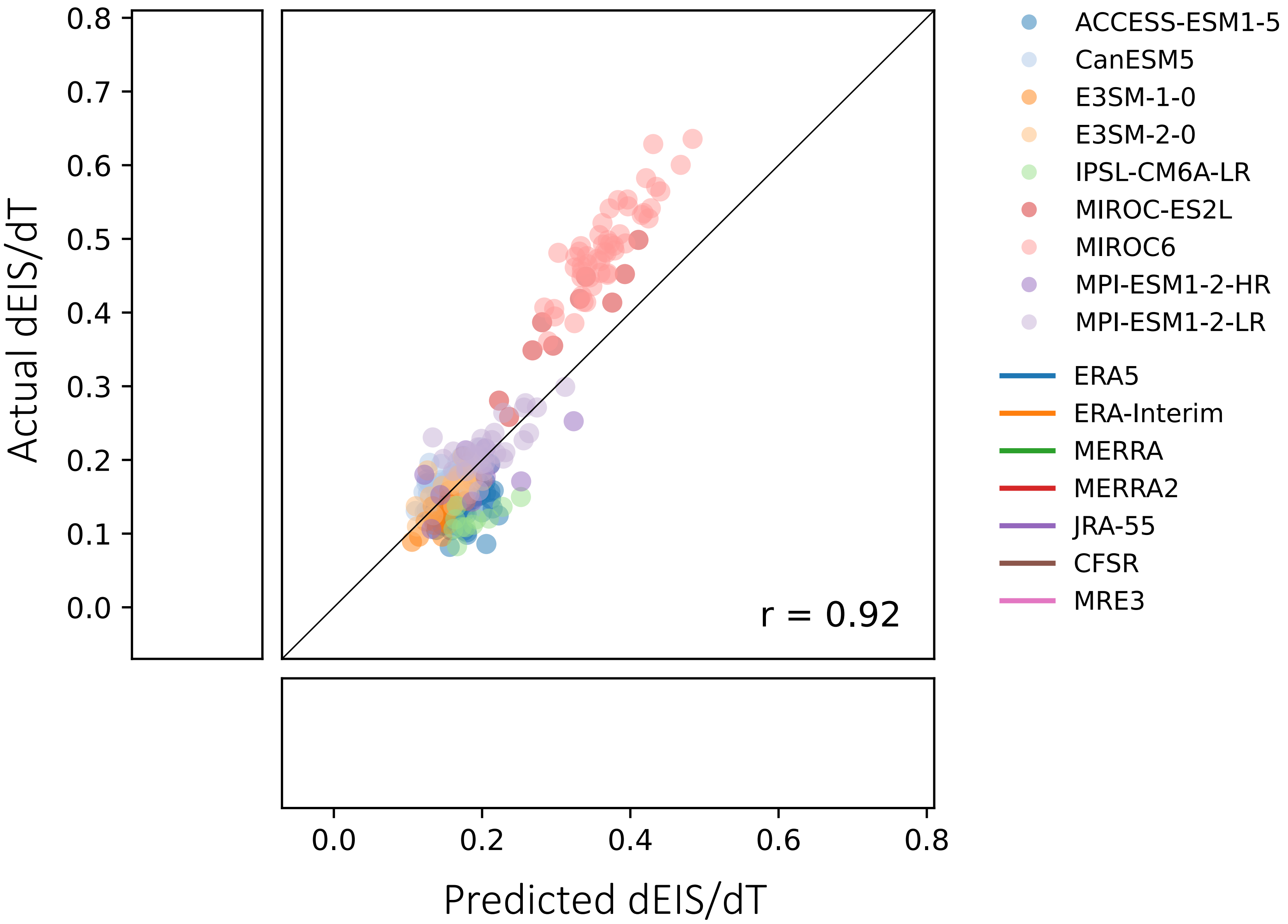

Actual dEIS/dT
Predicted dEIS/dT
0.0
0.1
0.2
0.3
0.4
0.5
0.6
0.7
0.8
0.0
0.2
0.4
0.6
0.8
r = 0.92
ACCESS-ESM1-5
CanESM5
E3SM-1-0
E3SM-2-0
IPSL-CM6A-LR
MIROC-ES2L
MIROC6
MPI-ESM1-2-HR
MPI-ESM1-2-LR
ERA5
ERA-Interim
MERRA
MERRA2
JRA-55
CFSR
MRE3

Results (2)

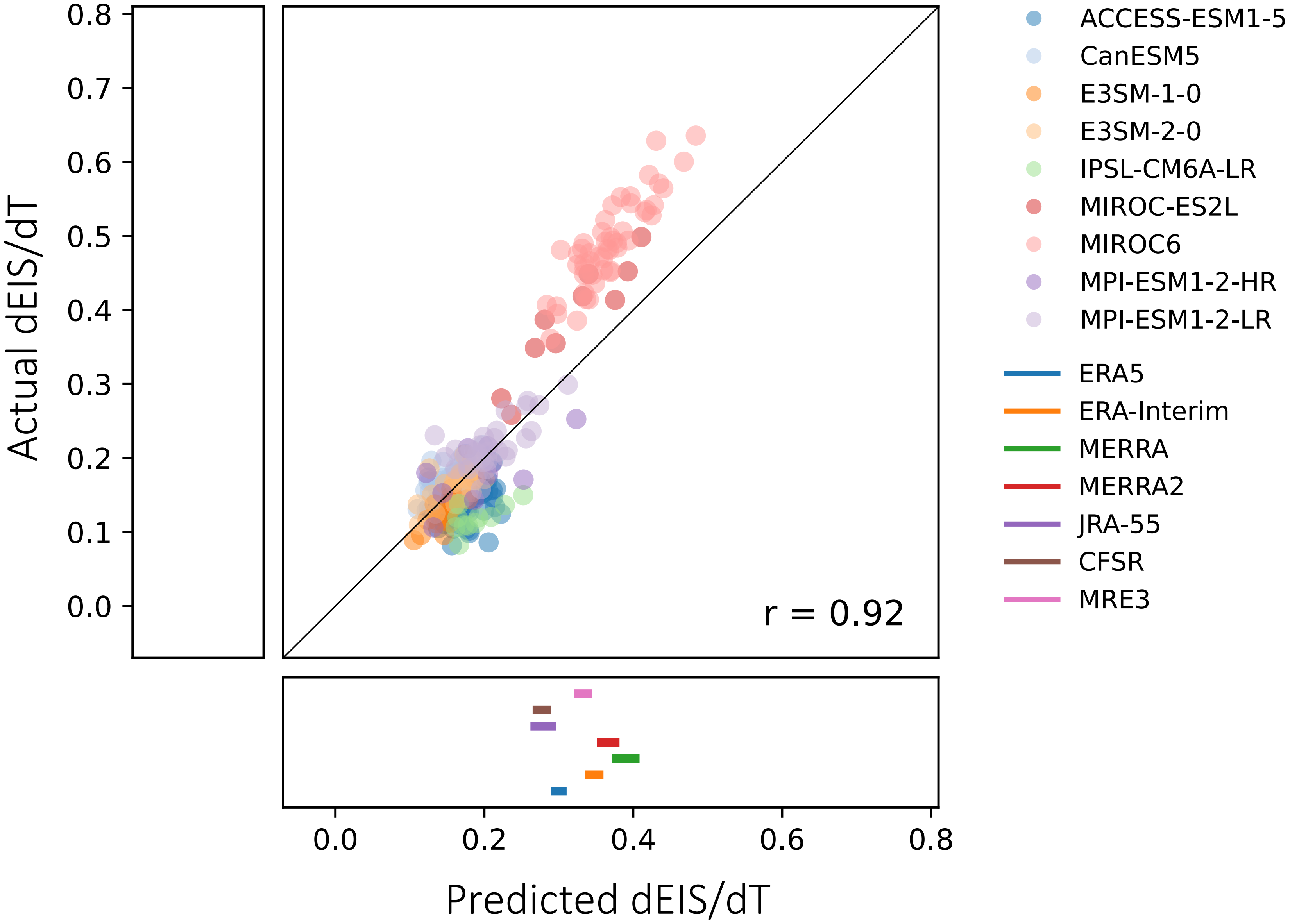

Actual dEIS/dT
Predicted dEIS/dT
0.0
0.1
0.2
0.3
0.4
0.5
0.6
0.7
0.8
0.0
0.2
0.4
0.6
0.8
r = 0.92
ACCESS-ESM1-5
CanESM5
E3SM-1-0
E3SM-2-0
IPSL-CM6A-LR
MIROC-ES2L
MIROC6
MPI-ESM1-2-HR
MPI-ESM1-2-LR
ERA5
ERA-Interim
MERRA
MERRA2
JRA-55
CFSR
MRE3

Results (2)

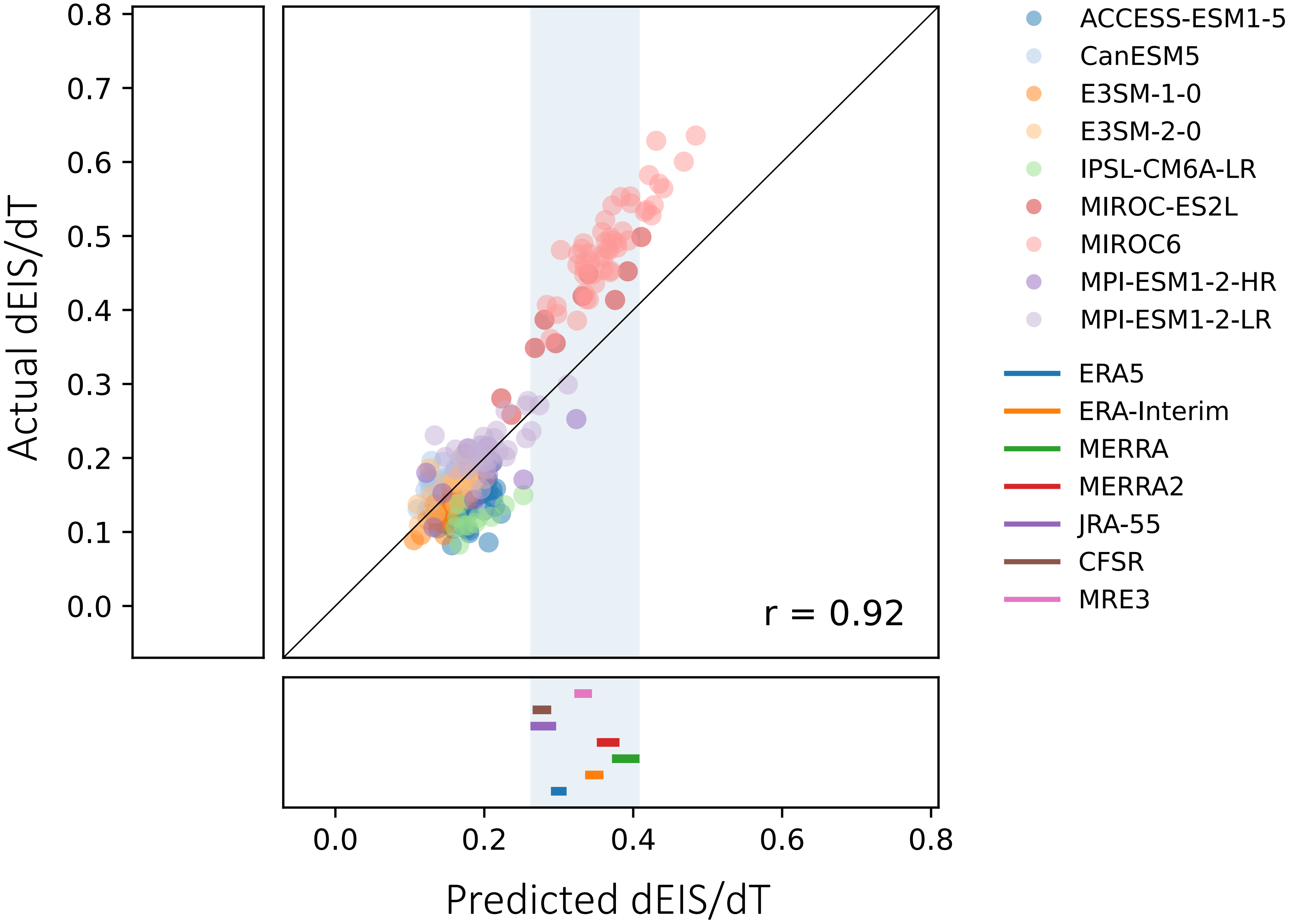

Actual dEIS/dT
0.8
0.7
0.6
0.5
0.4
0.3
0.2
0.1
0.0
r = 0.92
0.0
0.2
0.4
0.6
0.8
Predicted dEIS/dT
ACCESS-ESM1-5
CanESM5
E3SM-1-0
E3SM-2-0
IPSL-CM6A-LR
MIROC-ES2L
MIROC6
MPI-ESM1-2-HR
MPI-ESM1-2-LR
ERA5
ERA-Interim
MERRA
MERRA2
JRA-55
CFSR
MRE3

Results (2)

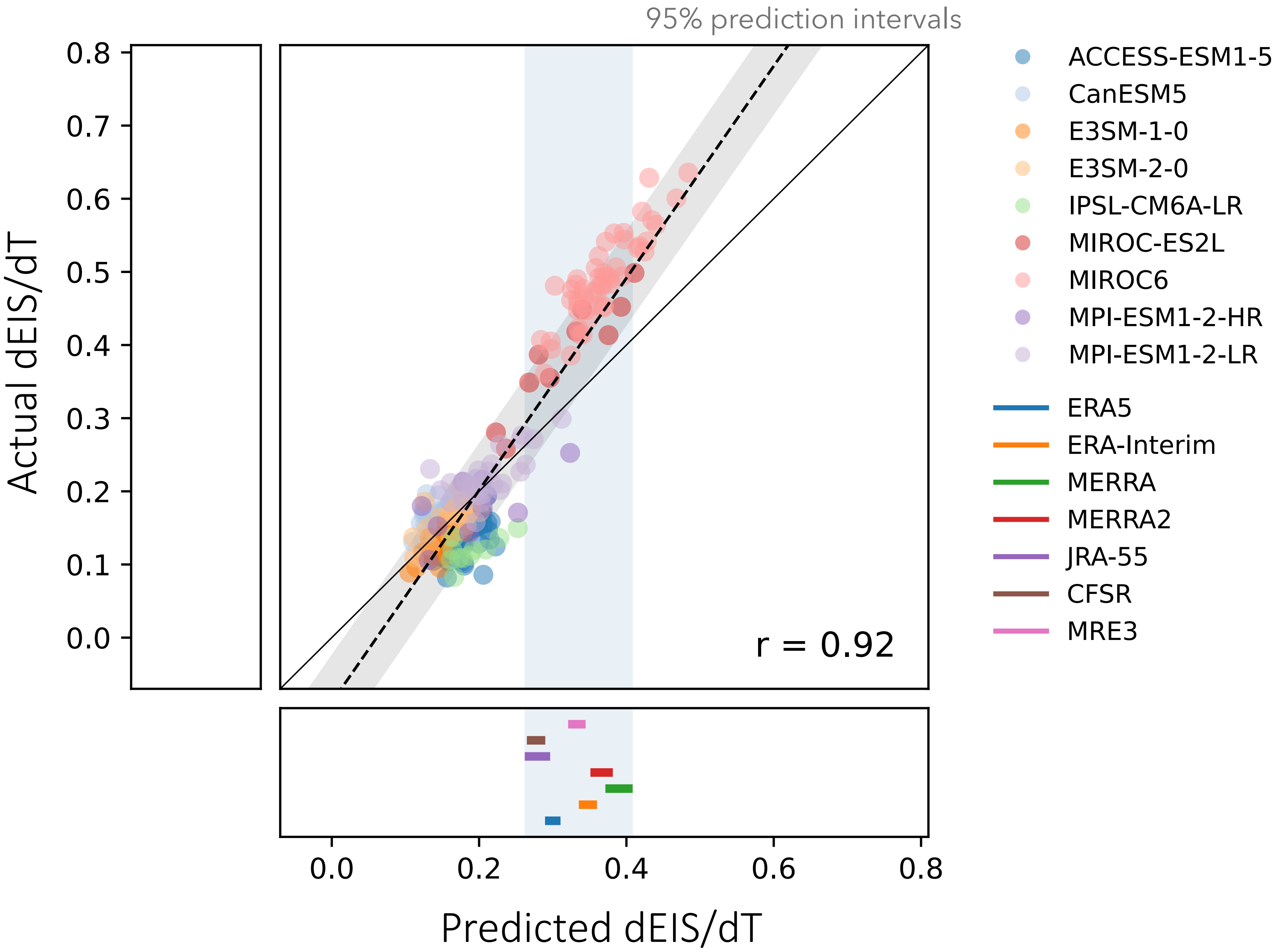

95% prediction intervals
Actual dEIS/dT
0.8
0.7
0.6
0.5
0.4
0.3
0.2
0.1
0.0
r = 0.92
0.0
0.2
0.4
0.6
0.8
Predicted dEIS/dT
ACCESS-ESM1-5
CanESM5
E3SM-1-0
E3SM-2-0
IPSL-CM6A-LR
MIROC-ES2L
MIROC6
MPI-ESM1-2-HR
MPI-ESM1-2-LR
ERA5
ERA-Interim
MERRA
MERRA2
JRA-55
CFSR
MRE3

Results (2)

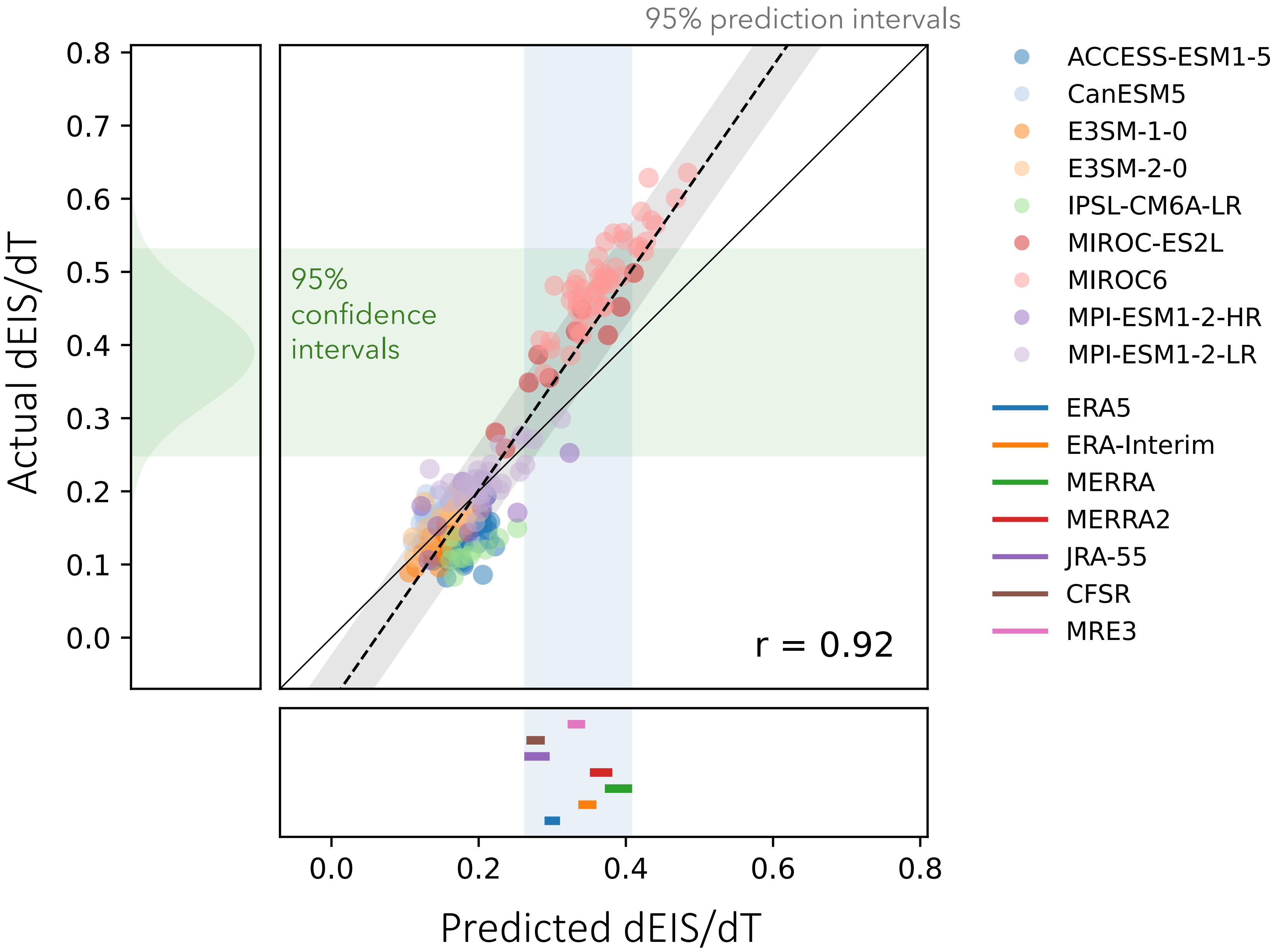
95% prediction intervals
95%
confidence
intervals
r = 0.92
Actual dEIS/dT
Predicted dEIS/dT
0.8
0.7
0.6
0.5
0.4
0.3
0.2
0.1
0.0
0.0
0.2
0.4
0.6
0.8
ACCESS-ESM1-5
CanESM5
E3SM-1-0
E3SM-2-0
IPSL-CM6A-LR
MIROC-ES2L
MIROC6
MPI-ESM1-2-HR
MPI-ESM1-2-LR
ERA5
ERA-Interim
MERRA
MERRA2
JRA-55
CFSR
MRE3

Results (2)

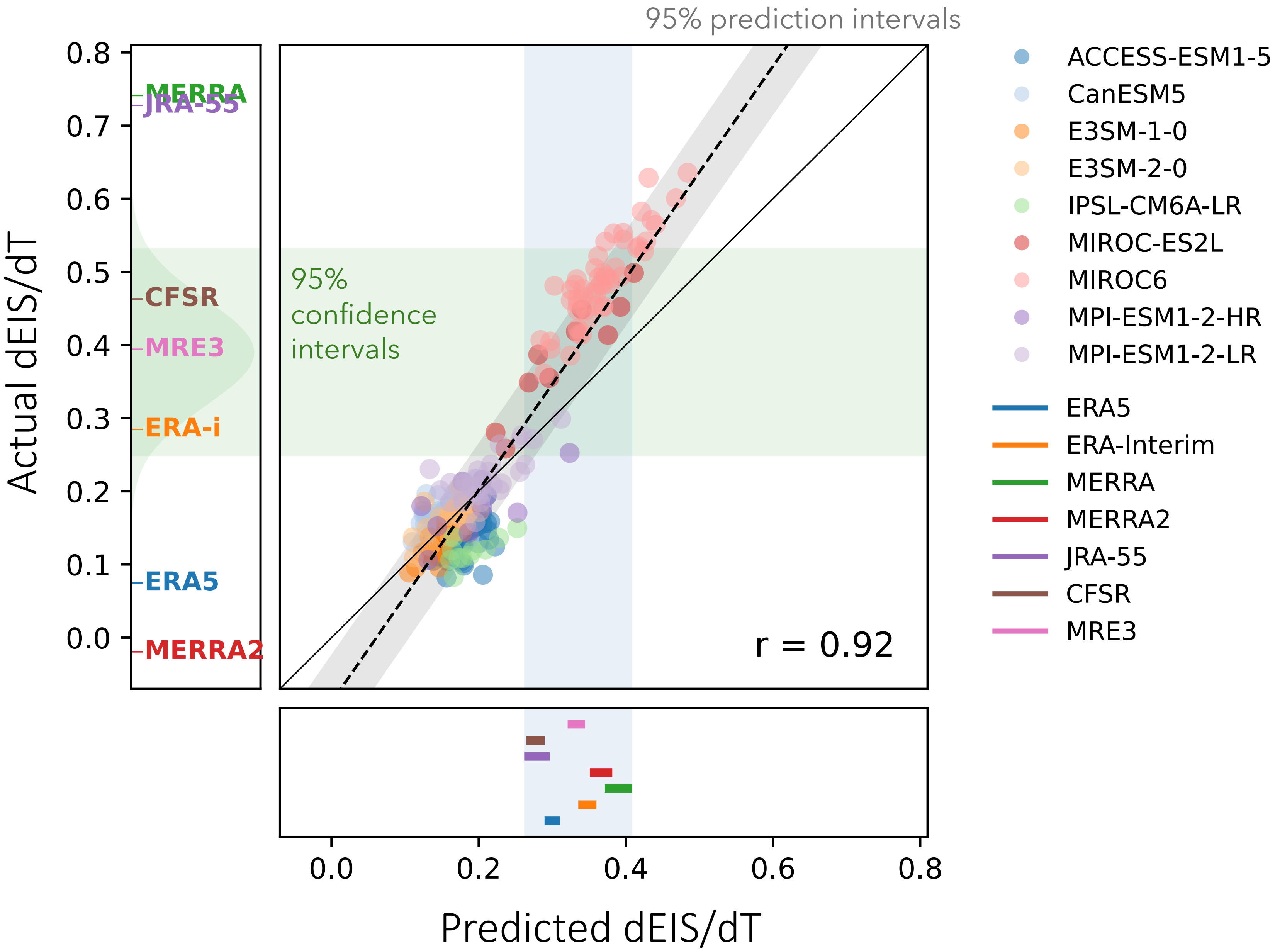
95% prediction intervals
0.8
0.7
0.6
0.5
0.4
0.3
0.2
0.1
0.0
MERRA
JRA-55
CFSR
MRE3
ERA-i
ERA5
MERRA2
Actual dEIS/dT
95%
confidence
intervals
r = 0.92
0.0
0.2
0.4
0.6
0.8
Predicted dEIS/dT
ACCESS-ESM1-5
CanESM5
E3SM-1-0
E3SM-2-0
IPSL-CM6A-LR
MIROC-ES2L
MIROC6
MPI-ESM1-2-HR
MPI-ESM1-2-LR
ERA5
ERA-Interim
MERRA
MERRA2
JRA-55
CFSR
MRE3

Results (3)

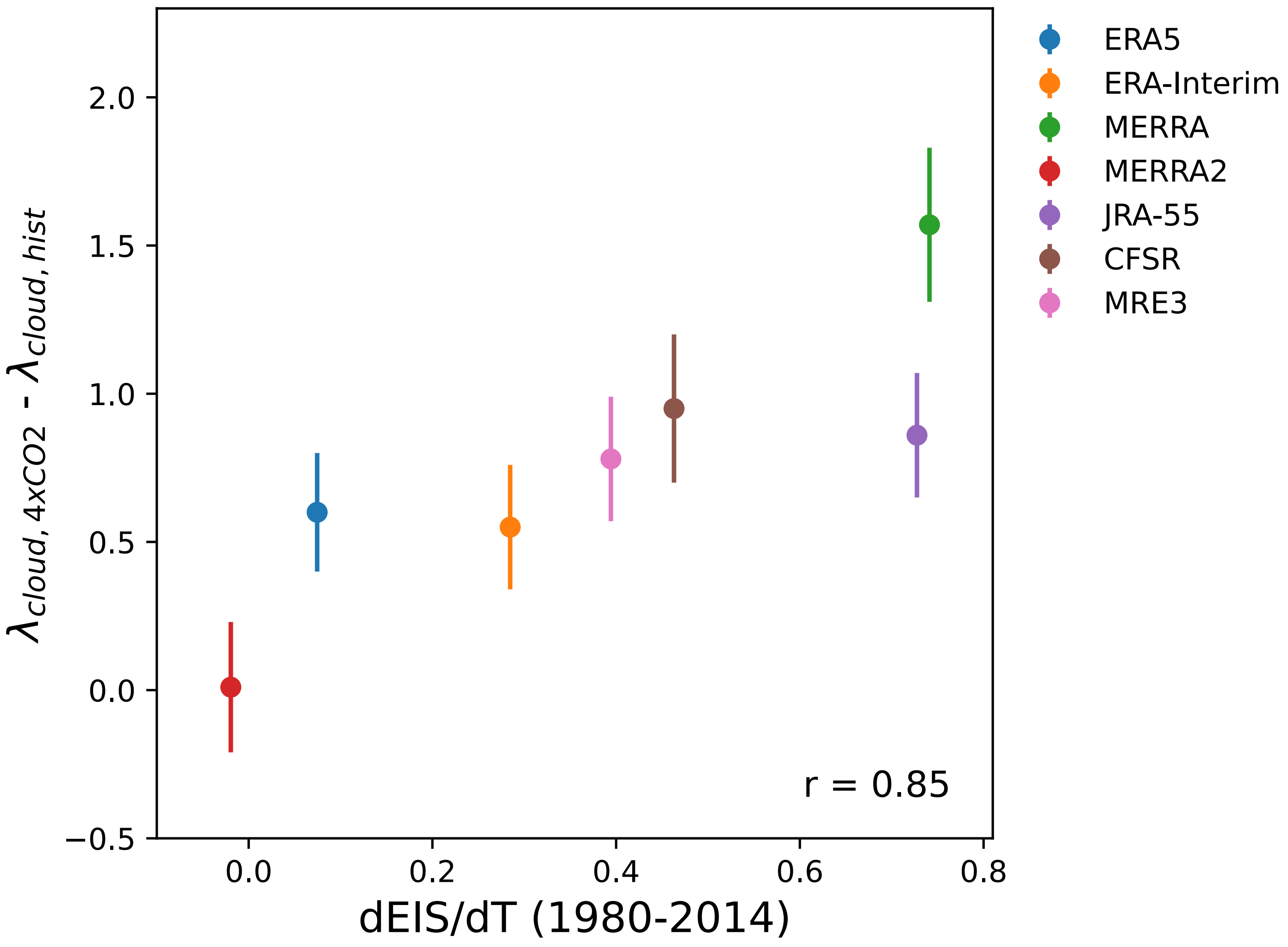

Cloud feedback pattern effect:

0.01 (MERRA2) to 1.57 (MERRA) W/m^2/K

Results (3)

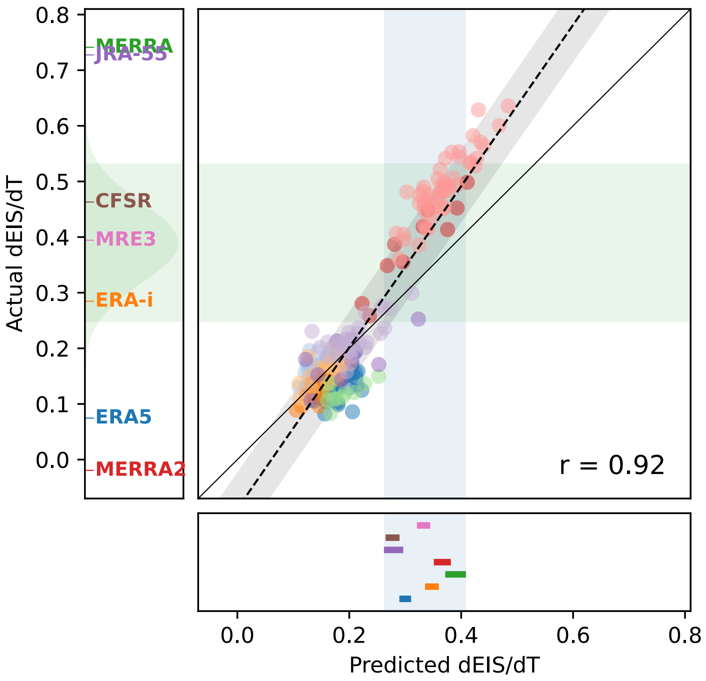

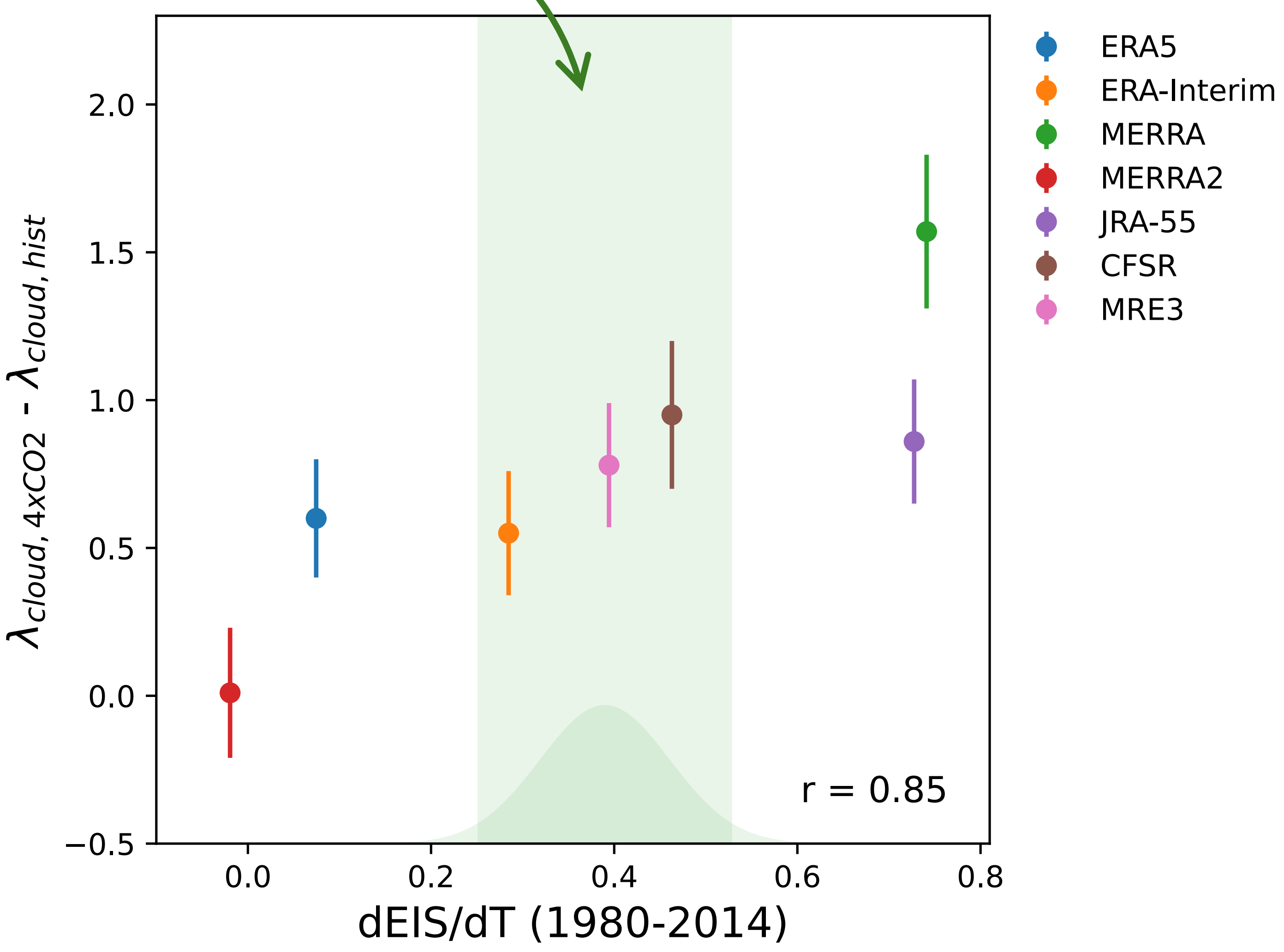

Cloud feedback pattern effect:

0.01 (MERRA2) to 1.57 (MERRA) W/m^2/K

Based on ML results →

0.55 (ERA-Interim) to 0.95 (CFSR) W/m^2/K

(implied percentage change = −74%)

Summary

- Observationally "constrained" estimates of the low-cloud feedback pattern effect over 1980-2014 vary widely (from roughly 0 to 1.6 $W/m^2/K$) primarily because **reanalyses strongly disagree on recent EIS trends**.
- We train a statistical learning algorithm on a suite of diverse GCMs to learn how EIS anomalies relate to surface temperature patterns, then apply it to observed surface warming patterns to estimate **observationally-constrained dEIS/dT values**.
- Our approach predicts dEIS/dT over 1980-2014 to range from **0.25 to 0.53 K/K**, roughly 1/3 of the raw spread across reanalyses.
- This implies a much tighter observational constraint on the low-cloud feedback pattern effect of **0.55 to 0.95 $W/m^2/K$**, and of the total pattern effect of about **1.6 to 2 $W/m^2/K$** for this period [using values from Myers et al (2023)]
- **Caveats:** The credibility of our results depends on GCMs realistically simulating the relationship between EIS and surface temperature patterns and on the accuracy of the ML approach to learn it. It also depends on the reliability of the surface temperature patterns derived from observational datasets.

Supplement

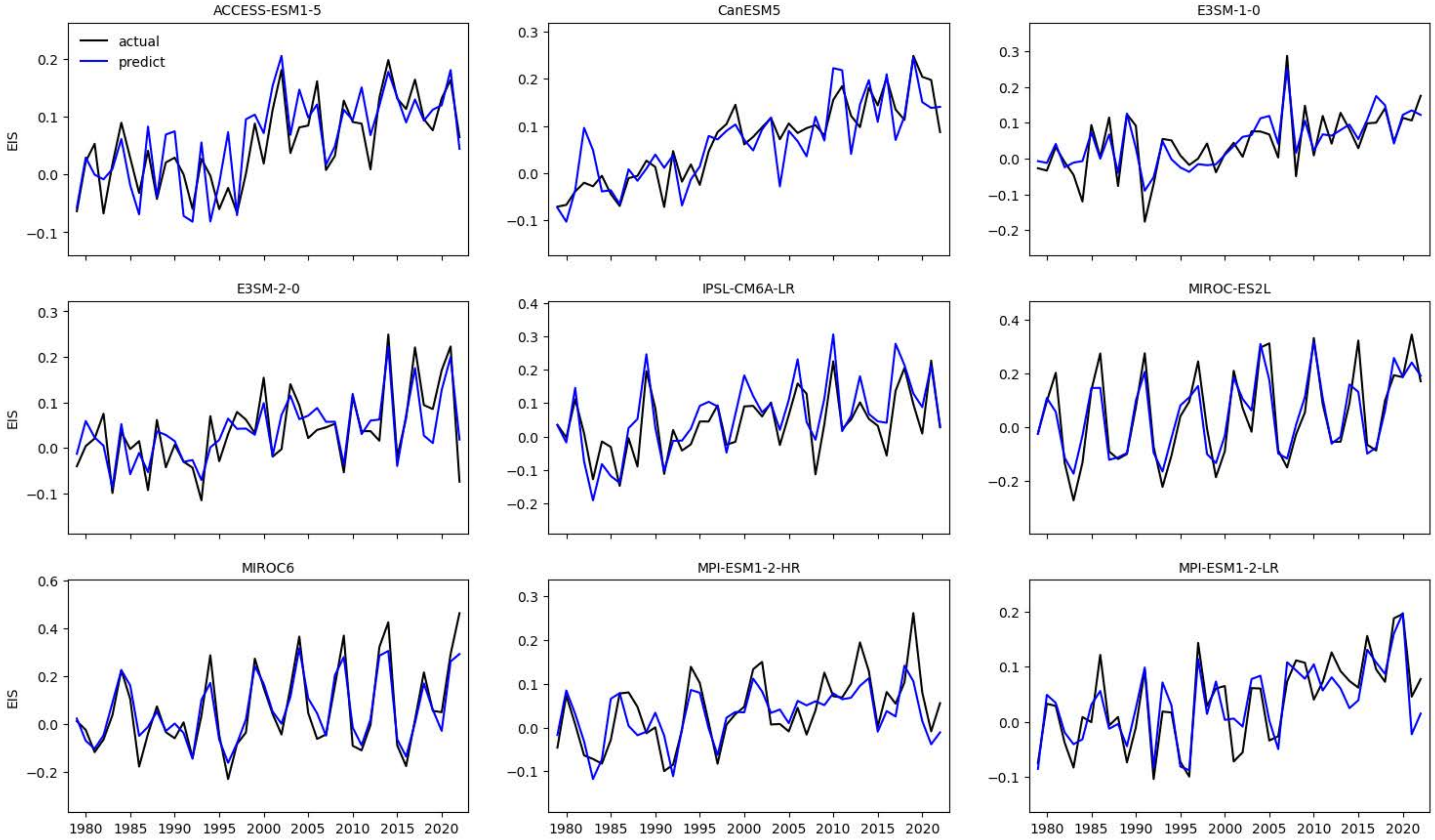
ACCESS-ESM1-5
CanESM5
E3SM-1-0
E3SM-2-0
IPSL-CM6A-LR
MIROC-ES2L
MIROC6
MPI-ESM1-2-HR
MPI-ESM1-2-LR
actual
predict
EIS

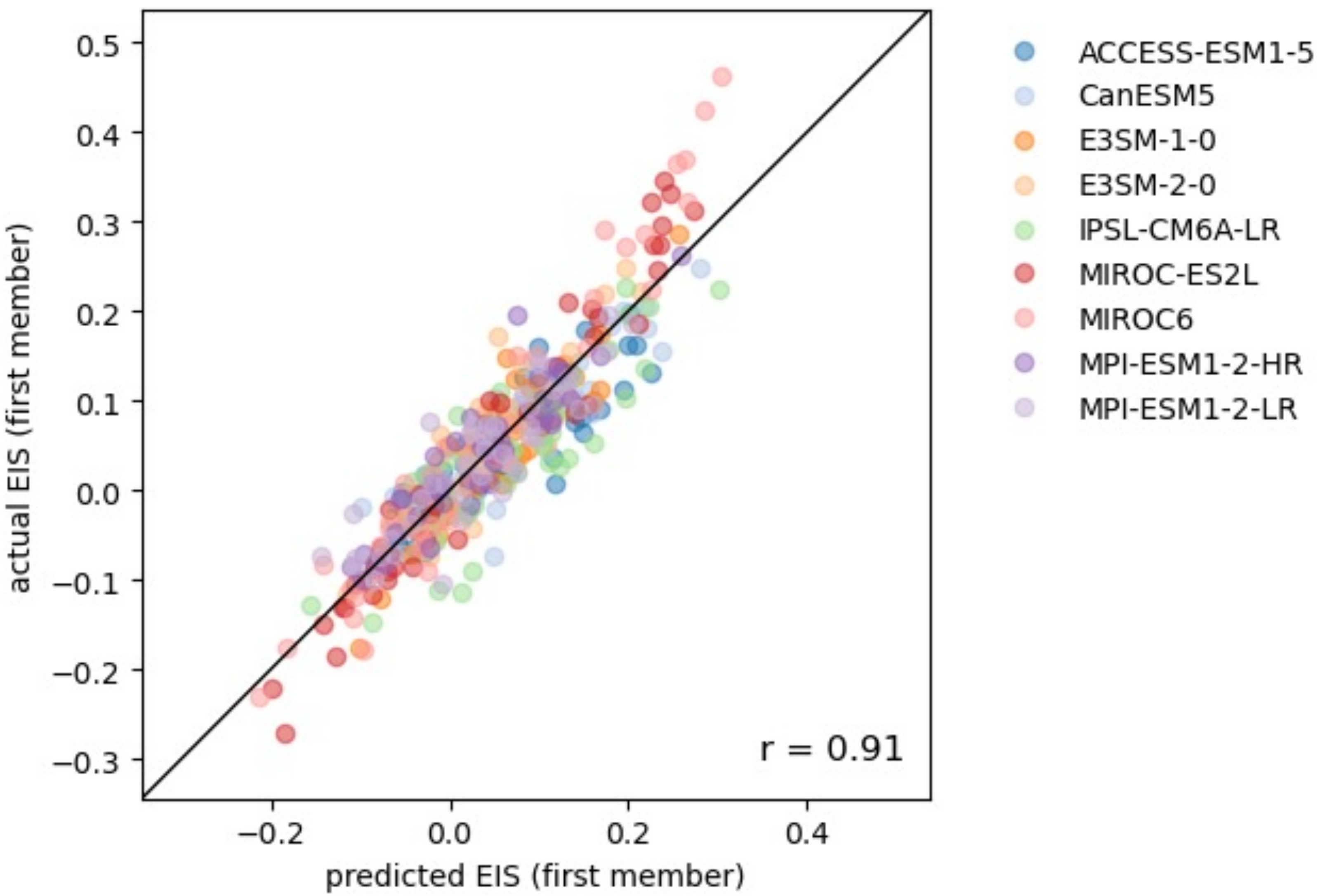
actual EIS (first member)
predicted EIS (first member)
0.5
0.4
0.3
0.2
0.1
0.0
−0.1
−0.2
−0.3
−0.2
0.0
0.2
0.4
r = 0.91
ACCESS-ESM1-5
CanESM5
E3SM-1-0
E3SM-2-0
IPSL-CM6A-LR
MIROC-ES2L
MIROC6
MPI-ESM1-2-HR
MPI-ESM1-2-LR

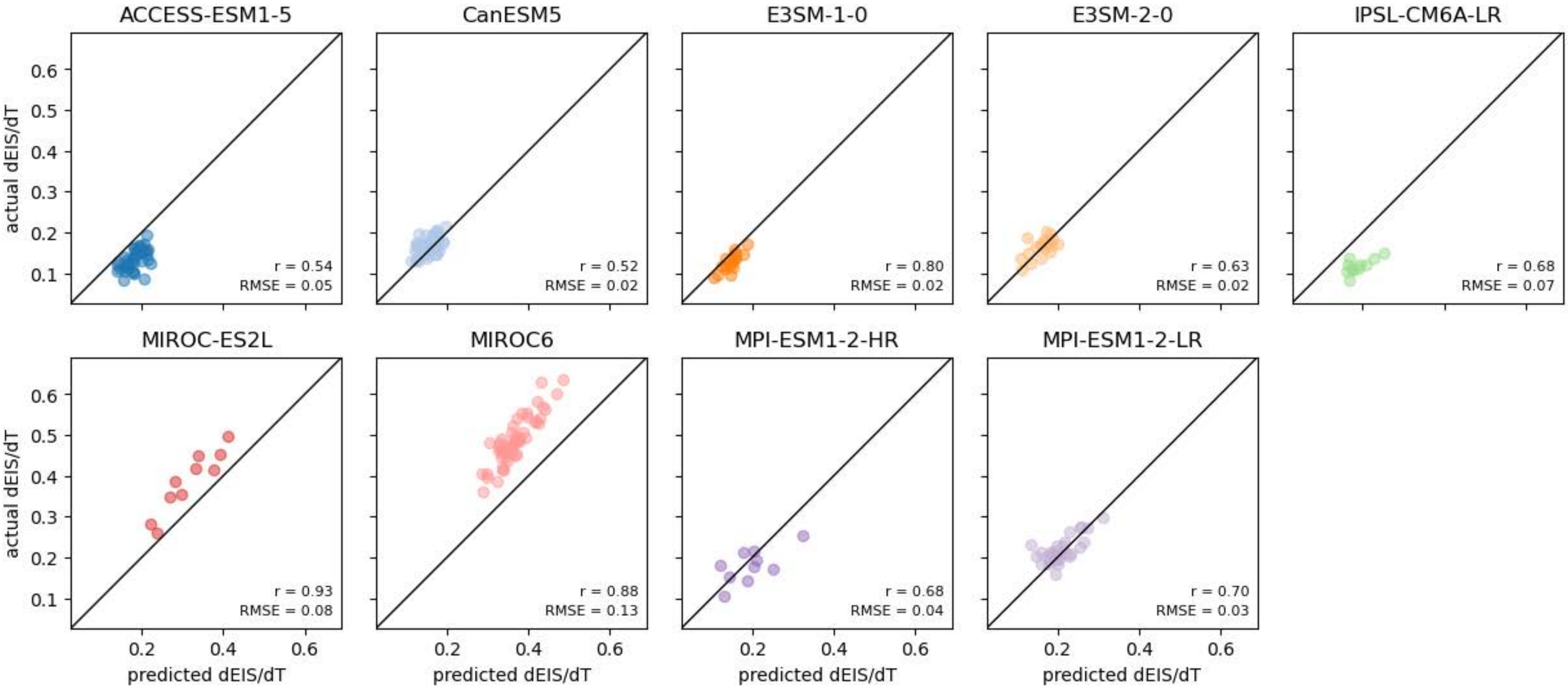
ACCESS-ESM1-5
CanESM5
E3SM-1-0
E3SM-2-0
IPSL-CM6A-LR
r = 0.54
RMSE = 0.05
r = 0.52
RMSE = 0.02
r = 0.80
RMSE = 0.02
r = 0.63
RMSE = 0.02
r = 0.68
RMSE = 0.07
MIROC-ES2L
MIROC6
MPI-ESM1-2-HR
MPI-ESM1-2-LR
r = 0.93
RMSE = 0.08
r = 0.88
RMSE = 0.13
r = 0.68
RMSE = 0.04
r = 0.70
RMSE = 0.03
actual dEIS/dT
predicted dEIS/dT
0.1
0.2
0.3
0.4
0.5
0.6

Predictor: Ts map
ML method: PLS regression

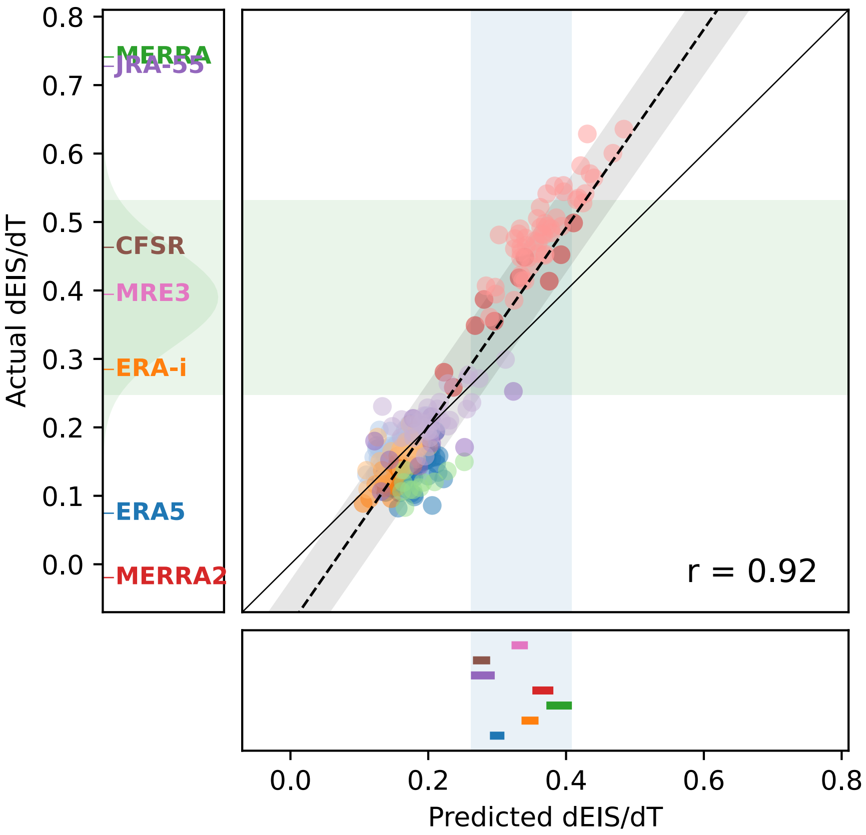

Predictor: SST percentile
ML method: PLS regression

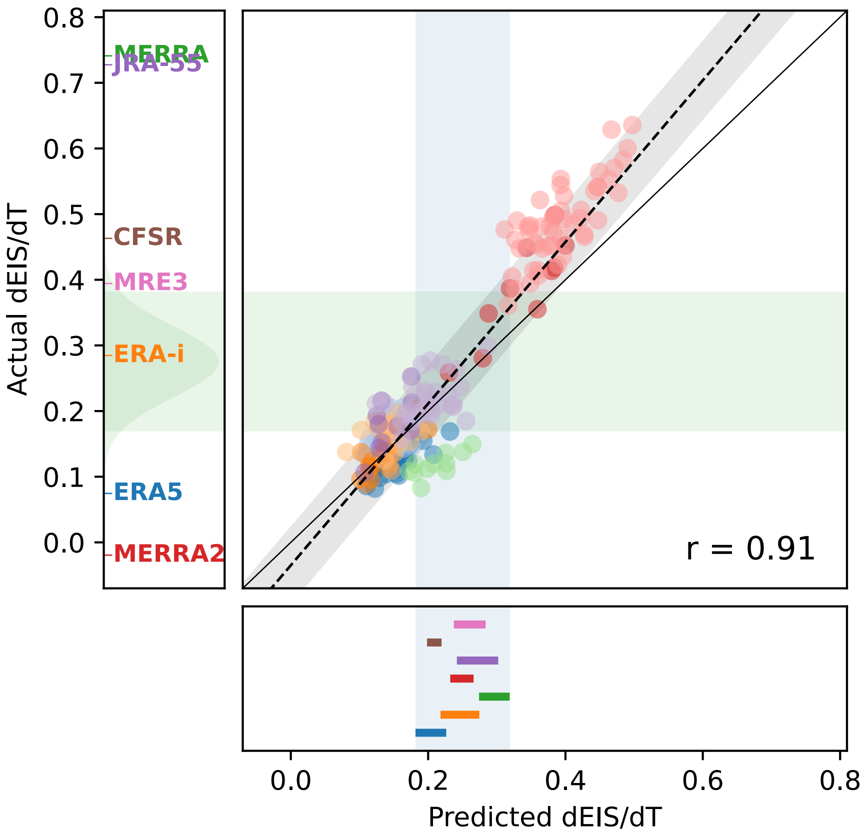

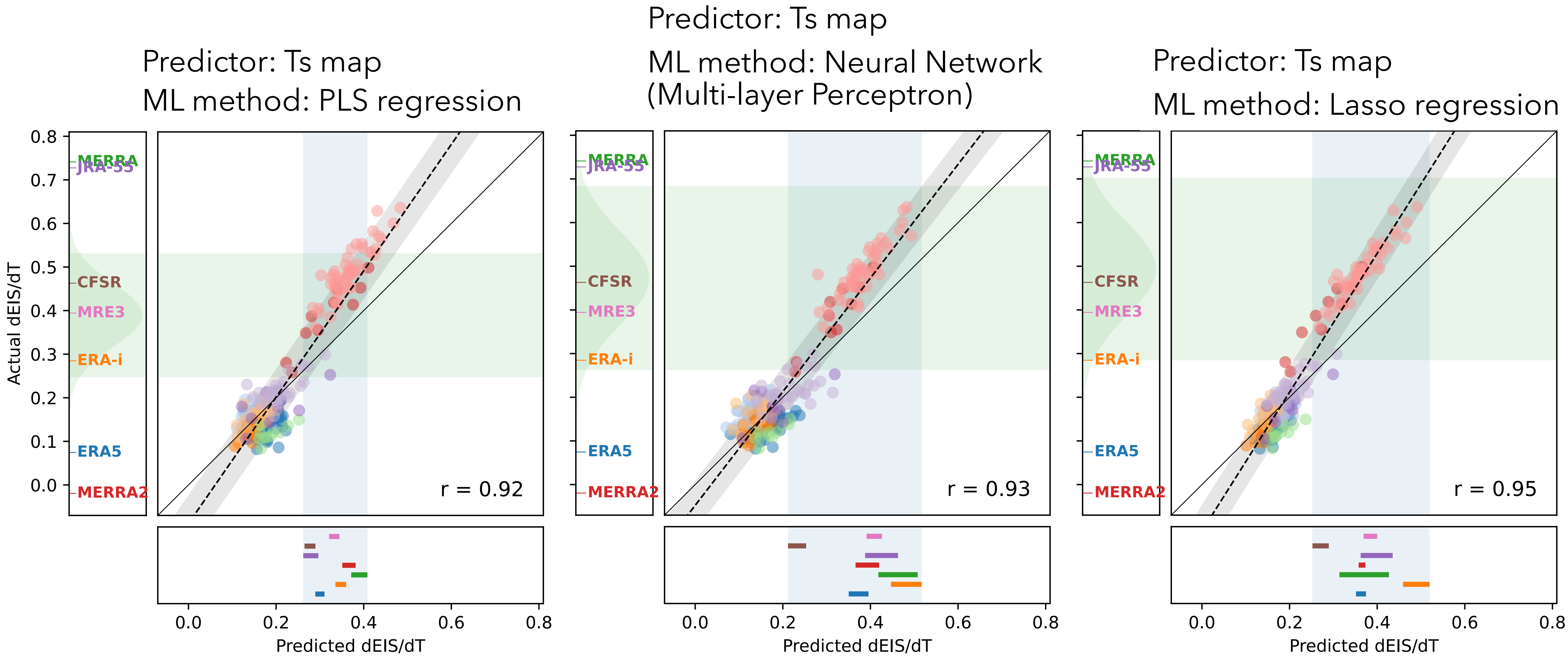

Predictor: Ts map
ML method: PLS regression
Predictor: Ts map
ML method: Neural Network (Multi-layer Perceptron)
Predictor: Ts map
ML method: Lasso regression
Actual dEIS/dT
MERRA
JRA-55
CFSR
MRE3
ERA-i
ERA5
MERRA2
r = 0.92
r = 0.93
r = 0.95
Predicted dEIS/dT

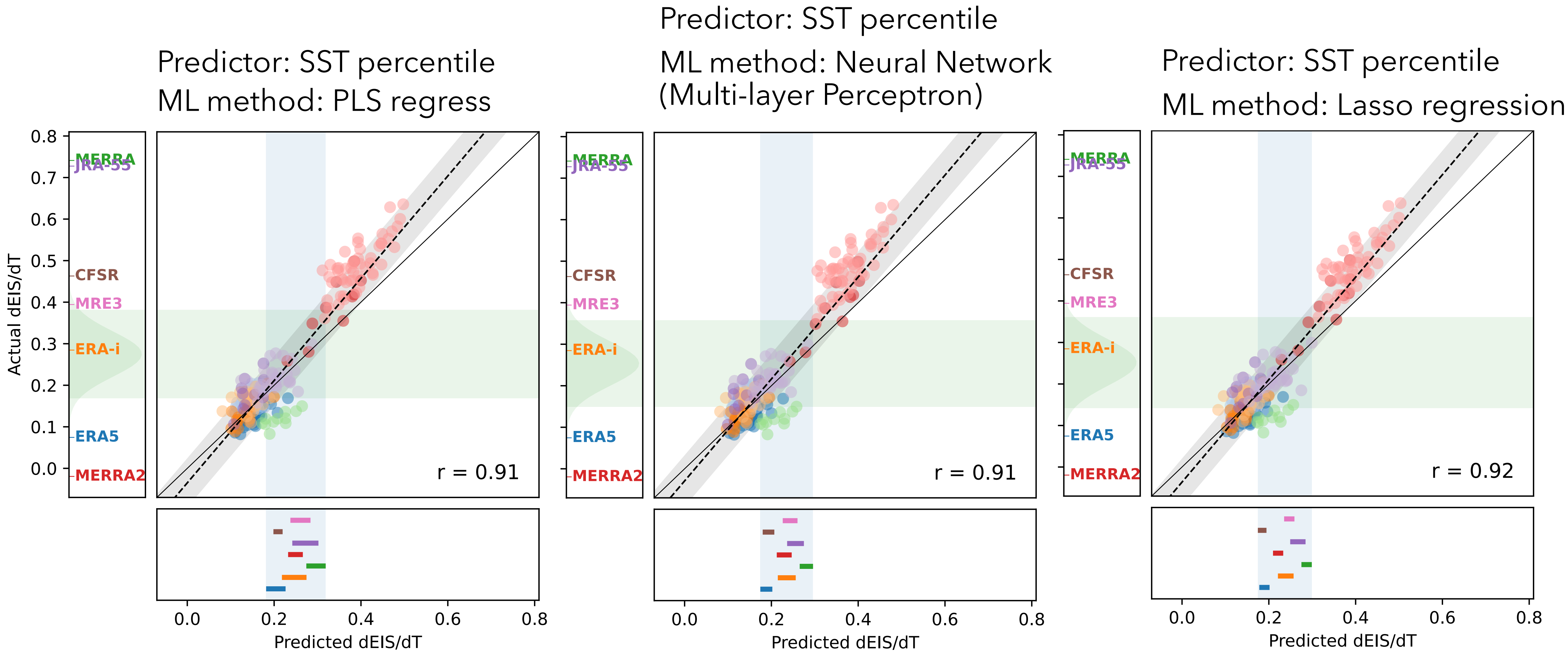

Predictor: SST percentile
ML method: PLS regress
Predictor: SST percentile
ML method: Neural Network
(Multi-layer Perceptron)
Predictor: SST percentile
ML method: Lasso regression
Actual dEIS/dT
MERRA
JRA-55
CFSR
MRE3
ERA-i
ERA5
MERRA2
r = 0.91
r = 0.91
r = 0.92
0.0
0.1
0.2
0.3
0.4
0.5
0.6
0.7
0.8
Predicted dEIS/dT

$$\Delta\lambda_{cloud} = \lambda_{cloud}^{4xCO2} - \lambda_{cloud}^{hist}$$

$$\lambda_{cloud}^{4xCO2} = \left[\frac{dR_{cloud}}{dT}\right]_{4xCO2} = \sum \left[\frac{\partial R_{cloud}}{\partial x_i}\right]_{obs} \left[\frac{dx_i}{dT}\right]_{4xCO2}$$

$$\lambda_{cloud}^{hist} = \left[\frac{dR_{cloud}}{dT}\right]_{hist} = \sum \left[\frac{\partial R_{cloud}}{\partial x_i}\right]_{obs} \left[\frac{dx_i}{dT}\right]_{hist}$$

Courtesy of Mark Zelinka

$$\Delta\lambda_{cloud} = \lambda_{cloud}^{4xCO2} - \lambda_{cloud}^{hist}$$

$$\lambda_{cloud}^{4xCO2} = \left[\frac{dR_{cloud}}{dT}\right]_{4xCO2} = \sum \boxed{\left[\frac{\partial R_{cloud}}{\partial x_i}\right]_{obs}} \boxed{\left[\frac{dx_i}{dT}\right]_{4xCO2}}$$

$$\lambda_{cloud}^{hist} = \left[\frac{dR_{cloud}}{dT}\right]_{hist} = \sum \boxed{\left[\frac{\partial R_{cloud}}{\partial x_i}\right]_{obs}} \boxed{\left[\frac{dx_i}{dT}\right]_{hist}}$$

SST | EIS

$\frac{\partial R_{cloud}}{\partial x_i}$ MODIS clouds + ERA5 meteo

$\left[\frac{dx_i}{dT}\right]_{4xCO2}$ CMIP GCMs

$\left[\frac{dx_i}{dT}\right]_{hist}$ ERA5 1980-2014

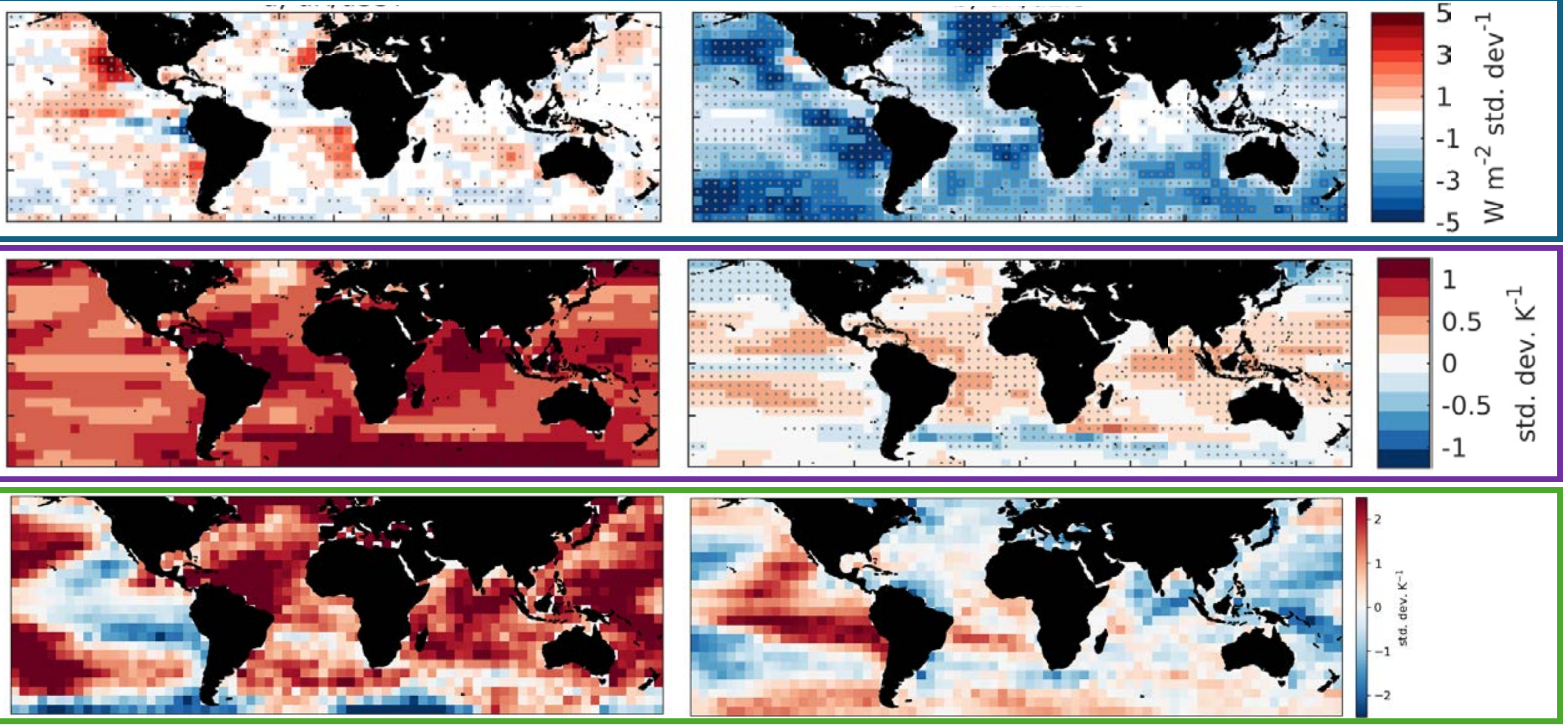

Scott et al. (2020)
Myers et al. (2021)
Myers et al. (2023)

Courtesy of Mark Zelinka